

The Power of Density Functional Theory for Materials Physics and Chemistry

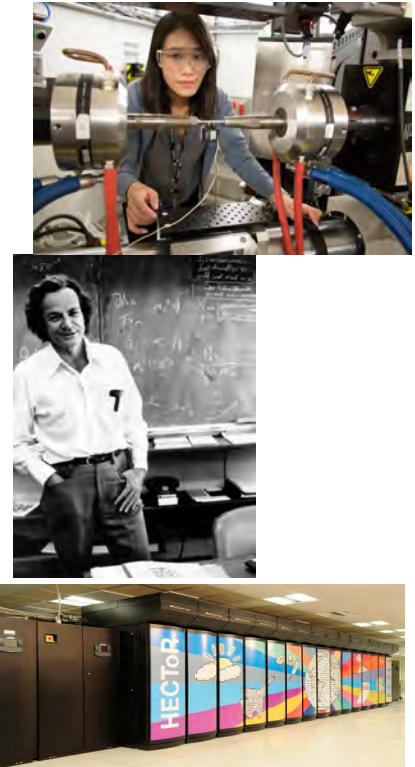
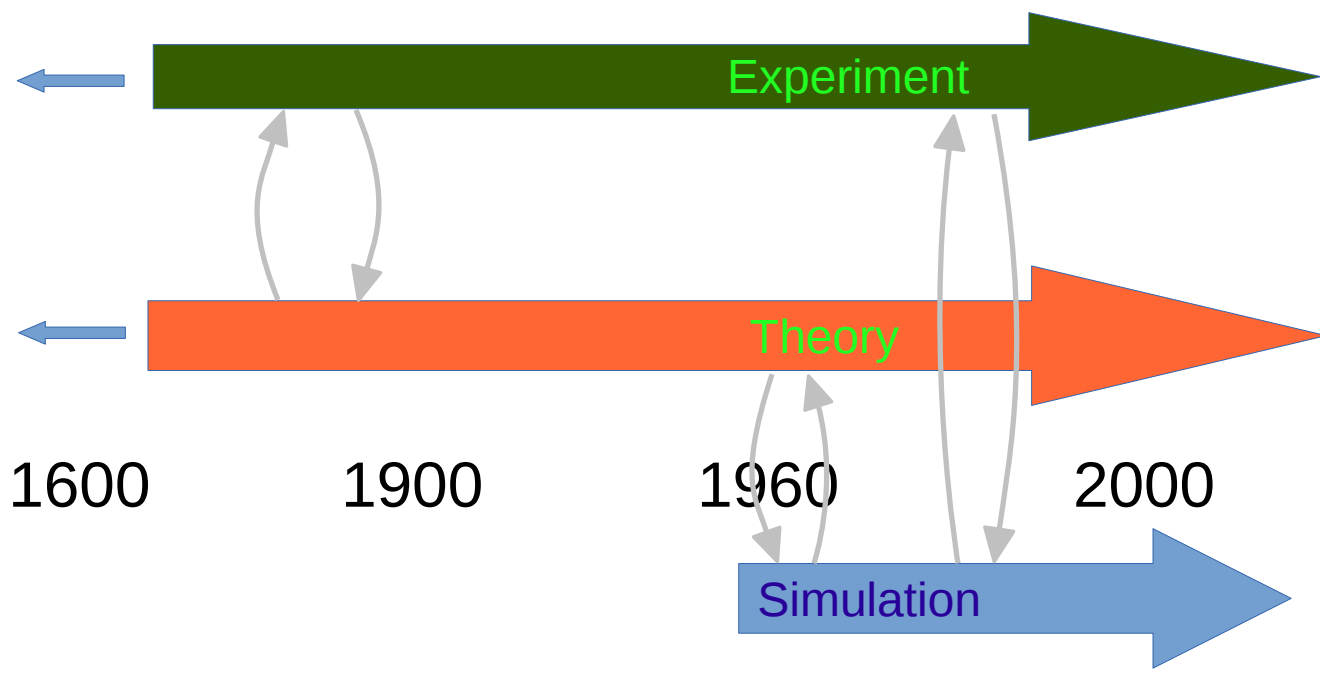
Date 12.09.19

Keith Refson



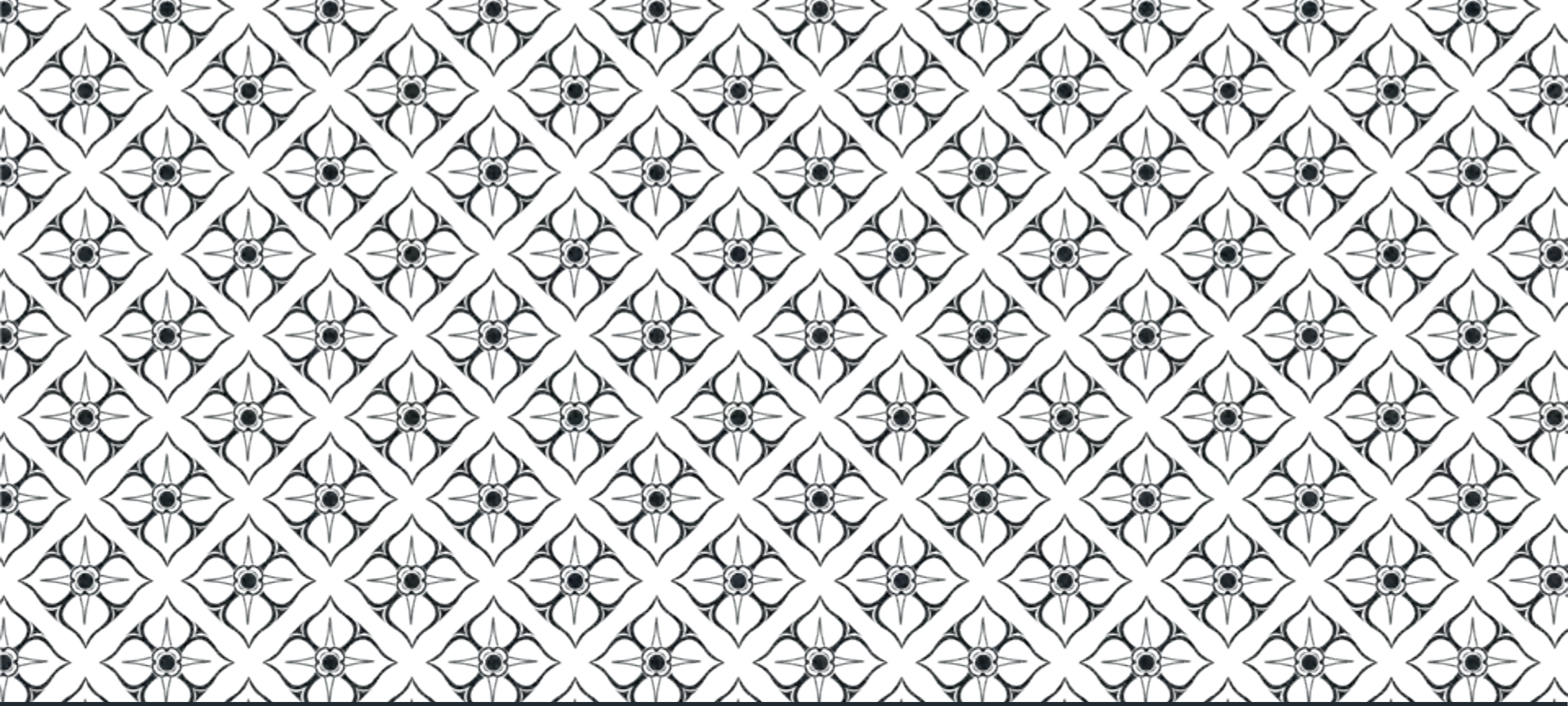
ROYAL
HOLLOWAY
UNIVERSITY
OF LONDON

Third mode of science

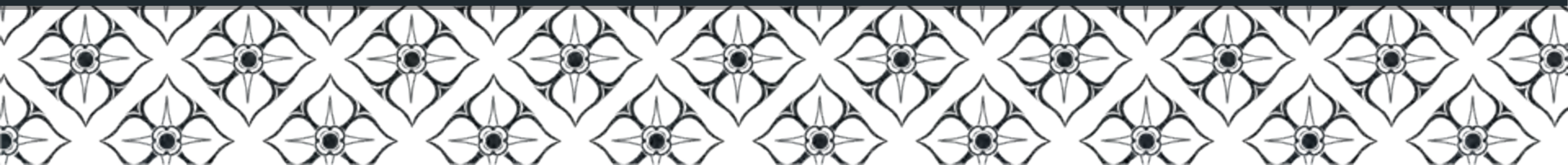


“During its spectacular rise, the computational has joined the theoretical and experimental branches of science, and is rapidly approaching its two older sisters in importance and intellectual respectability.”

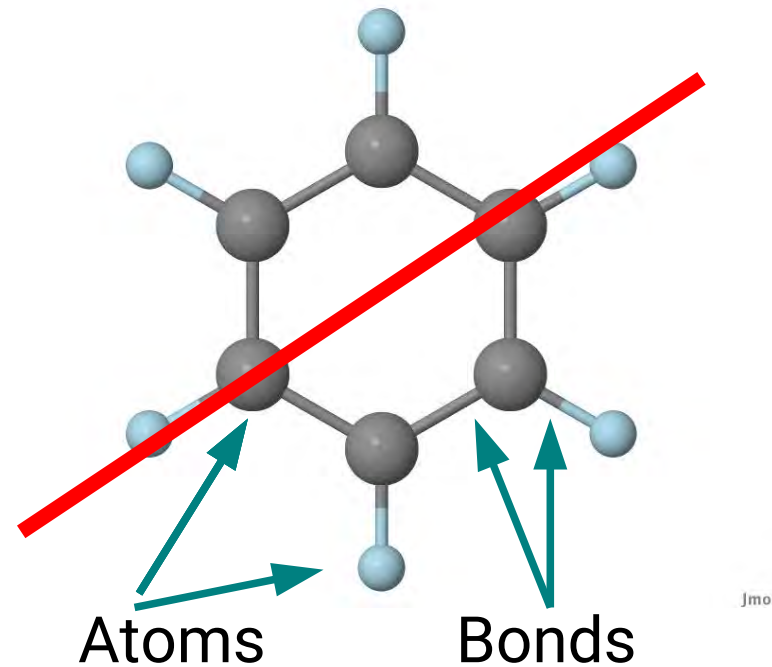
Peter D Lax, J. Stat. Phys. 43, 749 (1986)



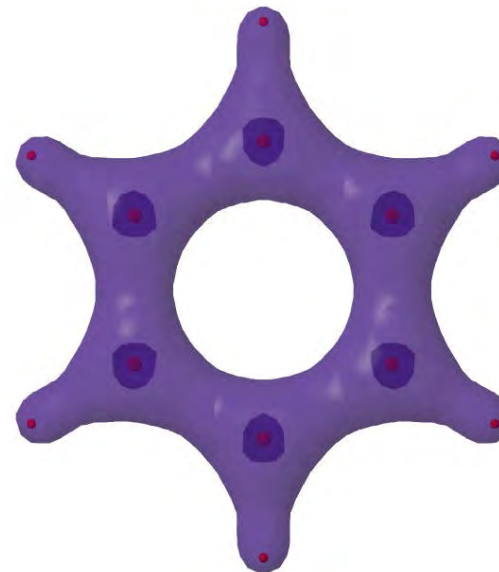
Quantum Mechanics and Density Functional Theory



The quantum Toolbox



Jmol



Jmol

Nuclei

Electrons

$$F = m \cdot a$$

$$\frac{-\hbar^2}{2m_e} \Psi + \hat{V} \Psi = E \Psi$$

The Theory of Everything

"The underlying physical laws necessary for the mathematical theory of a large part of physics and the whole of chemistry are thus completely known, and the difficulty is only that the application of these laws leads to equations much too complicated to be soluble."

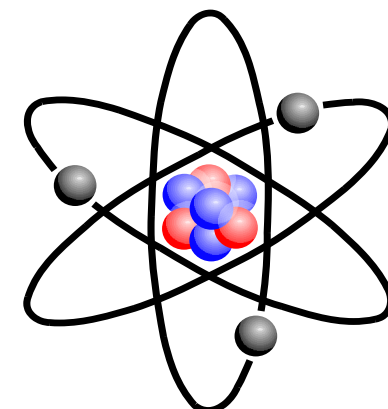
P.A.M. Dirac, Proceedings of the Royal Society **A123**, 714 (1929)

Why?

Each electron interacts with the nucleus
Every electron also interacts with every other electron.

In Lithium ($Z=3$) there are **3 e-e interactions** to consider.
In Boron ($Z=5$) there are **10 e-e interactions** to consider.
In Iron ($Z=26$) there are **325 e-e interactions** to consider.
In Uranium ($Z=92$) there are **4186 e-e interactions** to consider.

.. and that's just isolated atoms. We need to model crystals and molecules containing hundreds of atoms.

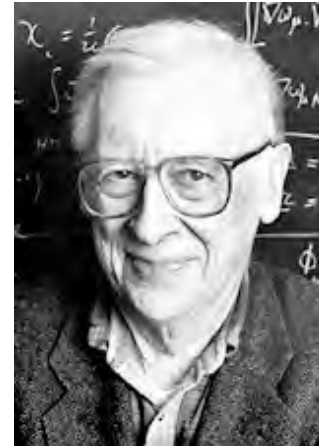


QM of multi-electron atoms still too complex to solve on
Powerful supercomputers in 2019 (and foreseeable future)..

Approximate quantum mechanics



Walter Kohn 1923-2016



John Pople 1925-2004

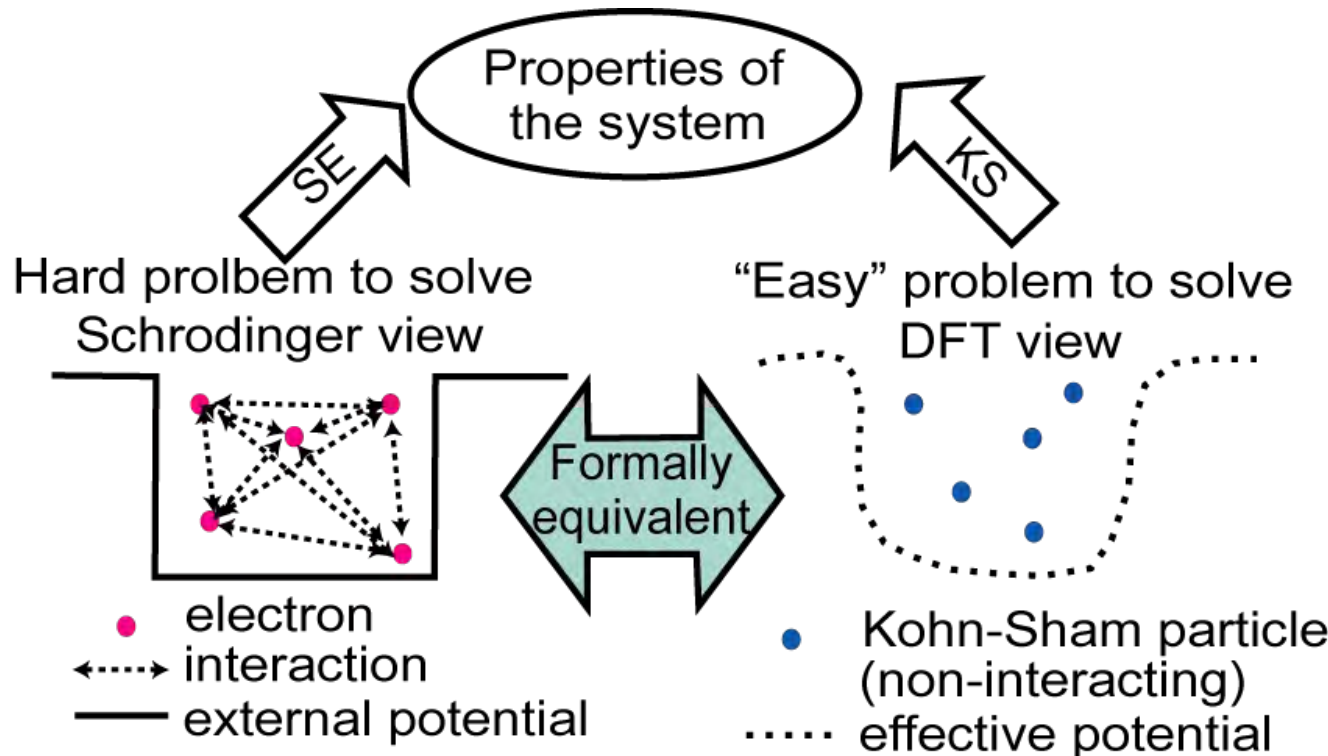
The Nobel Prize in Chemistry 1998 was divided equally between Walter Kohn "for his development of the **density-functional theory**" and John A. Pople "for his development of computational methods in **quantum chemistry**".

Key developments dating back to 1960s and 70s were approximate quantum theories which were nevertheless "good enough".

Density Functional Theory- Local Density Approximation

Hartree-Fock approximation, MP2, CI, CCSD(S,T)

Density Functional Theory



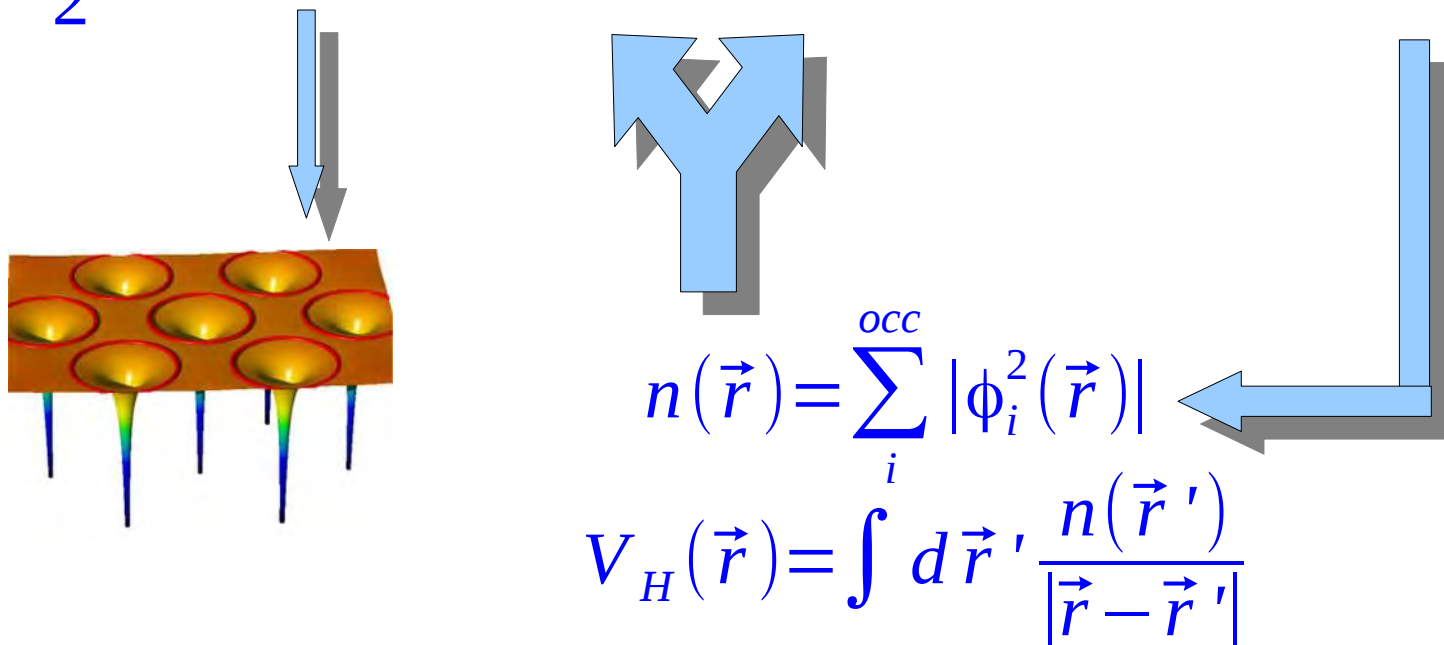
Approximate e-e interaction with

- local density approximation (LDA)
- generalized gradient approximation (GGA)
- Hybrids, DMFT, GW, ...

Modified from Mattsson et al., (2005)
Modeling. Simul. Mater. Sci. Eng. 13, R1.

Kohn-Sham equations

$$\left\{ \frac{1}{2} \nabla^2 + V_{\text{ext}}(\vec{r}) + V_H(\vec{r}) + V_{\text{xc}}([n(\vec{r})]) \right\} \phi_i(\vec{r}) = \epsilon_i \phi_i(\vec{r})$$



Self-consistent solution required.

LDA and GGAs

LDA

$$V_{xc}[n] \approx V_{xc}(n(\vec{r}))$$

$$V_{xc} \equiv \frac{\delta E_{xc}[n]}{\delta n(\vec{r})}$$

Parameterized from uniform electron gas

- Cohesive energies $\sim 1\text{eV}$ too large
- lattice parameters and bond lengths -1-2%
- Band gaps too small
- Hund's rule for open shells not always obeyed
- Van der Waals forces not included

GGAs

$$V_{xc}[n] \approx V_{xc}(n(\vec{r}), \nabla n(\vec{r}))$$

e.g. PBE, PW91, BLYP, ...

Parameterized from non-uniform electron gas and atoms

- Cohesive energies error of $\sim 100\text{ meV}$
- lattice parameters and bond lengths -1-2%
- Band gaps too small
- Hund's rule for open shells not always obeyed
- Van der Waals forces not included

Meta GGAs and Hybrids

Meta-GGA $V_{xc}[n] \approx V_{xc}(n(\vec{r}), \nabla n(\vec{r}), \tau_s(\vec{r}))$ $\tau_s(\vec{r}) = \frac{1}{2} \sum_{mk} |\nabla \phi_{mk}(\vec{r})|^2$

Added dependency on kinetic-energy density

- Early forms (TPSS) not fully self-consistent.
- SCAN & rSCAN fitted to exact results and QMC.
- lattice parameter error $\sim 0.007\text{\AA}$
- Self-interaction error still present (Hund's rule not always obeyed)
Cohesive energies accurate to $\sim 30\text{ meV}$
- Van der Waals forces still not included

Hybrids

$$E_{xc}^{PBE0} \equiv \frac{3}{4} E_x^{PBE} + \frac{1}{4} E_x^{HF} + E_c^{PBE}$$

e.g. PBE0, B3LYP, HSE06...

Linear admixture of DFT and Hartree-Fock exchange

- Cohesive energies and lattice parameters slightly better than GGAs
- Partially self-interaction corrected – band gaps improved
- Hund's rule for open shells obeyed
- Van der Waals forces not included

Plane-waves and pseudopotentials

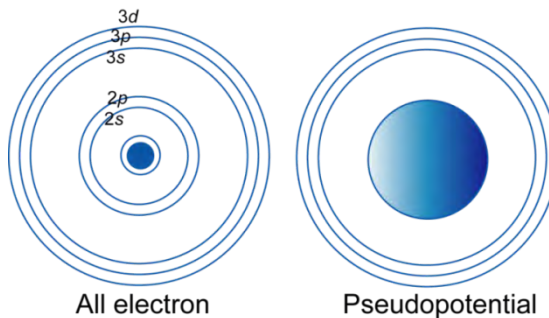
Plane-wave basis set

$$\psi_{n,\mathbf{k}}(\mathbf{r}) = u_{n,\mathbf{k}}(\mathbf{r})e^{i\mathbf{k}\mathbf{r}},$$

$$u_{n,\mathbf{k}}(\mathbf{r}) = \frac{1}{\Omega^{1/2}} \sum_{\mathbf{G}} C_{\mathbf{G}n\mathbf{k}} e^{i\mathbf{G}\mathbf{r}}$$

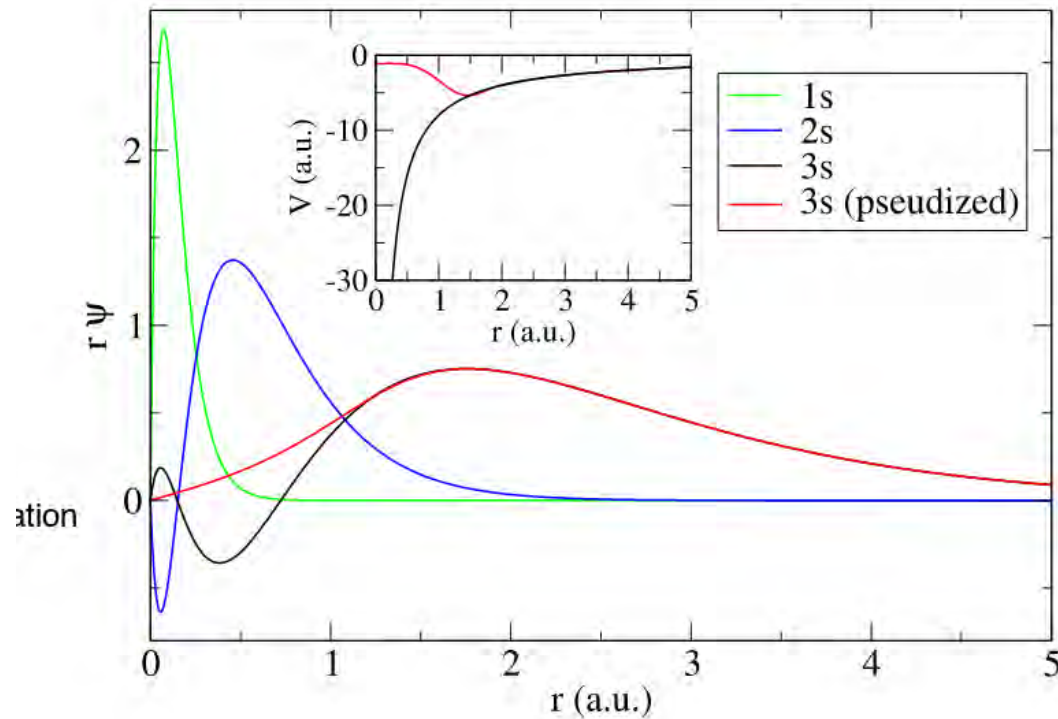
- Well-adapted for crystalline and solid/liquid modelling
- Systematic control of basis set convergence

Pseudopotential for ionic interactions



- “All electron” method but frozen core.
- Retain chemically relevant valence electrons
- Good scaling/large systems

Pseudopotentials

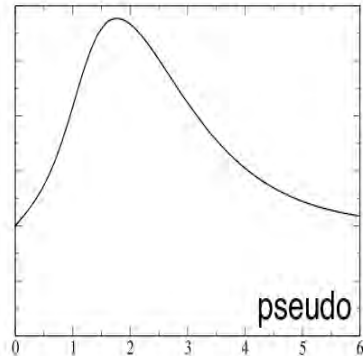


Valence orbitals determined by DFT calculation on isolated atom
Pseudization finds potential which retains large- r form
N.B. use relativistic atom solver to include relativity in plane-wave calc.
- correct treatment of heavy atoms.

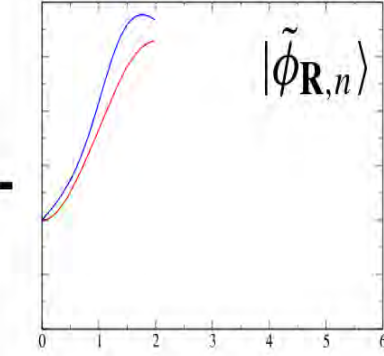
PAW

$$|\Psi\rangle = \mathcal{T}|\tilde{\Psi}\rangle$$

all-electron

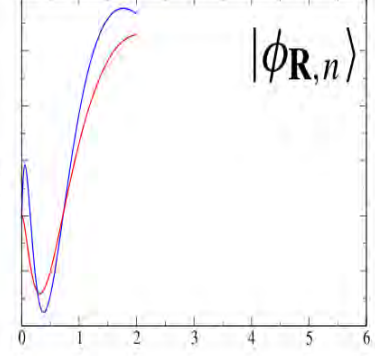


pseudo

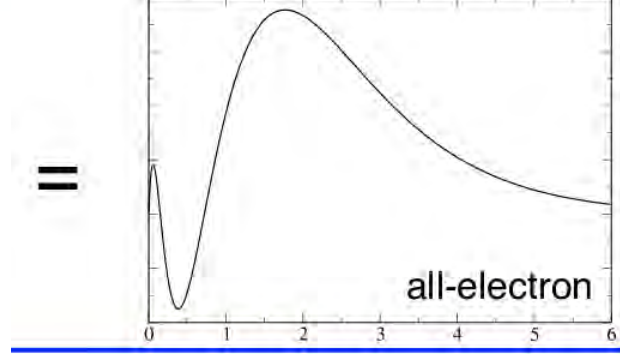


$$\mathcal{T} = \mathbf{1} + \sum_{\mathbf{R},n} [|\phi_{\mathbf{R},n}\rangle - |\tilde{\phi}_{\mathbf{R},n}\rangle] \langle \tilde{p}_{\mathbf{R},n}|$$

+



=



PAW is extension of pseudopotential method.

Restores atomic nodal form of plane-wave orbitals near nucleus

Sometimes called “all-electron”, but core electrons not included!

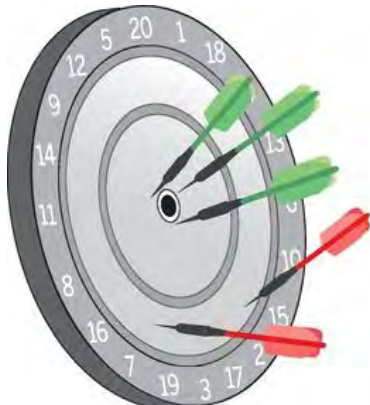
The Delta Project

RESEARCH ARTICLE

DFT METHODS

Reproducibility in density functional theory calculations of solids

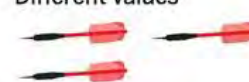
Kurt Lejaeghere,^{1*} Gustav Bihlmayer,² Torbjörn Björkman,^{3,4} Peter Blaha,⁵ Stefan Blügel,² Volker Blum,⁶ Damien Caliste,^{7,8} Ivano E. Castelli,⁹ Stewart J. Clark,¹⁰ Andrea Dal Corso,¹¹ Stefano de Gironcoli,¹¹ Thierry Deutsch,^{7,8} John Kay Dewhurst,¹² Igor Di Marco,¹³ Claudia Draxl,^{14,15} Marcin Dulak,¹⁶ Olle Eriksson,¹³ José A. Flores-Livas,¹² Kevin F. Garrity,¹⁷ Luigi Genovese,^{7,8} Paolo Giannozzi,¹⁸ Matteo Giantomassi,¹⁹ Stefan Goedecker,²⁰ Xavier Gonze,¹⁹ Oscar Gränäs,^{13,21} E. K. U. Gross,¹² Andris Gulans,^{14,15} Françoise Gygi,²² D. R. Hamann,^{23,24} Phil J. Hasnip,²⁵ N. A. W. Holzwarth,²⁶ Diana Iușan,¹³ Dominik B. Jochym,²⁷ François Jollet,²⁸ Daniel Jones,²⁹ Georg Kresse,³⁰ Klaus Koepenik,^{31,32} Emine Küçükbenli,^{9,11} Yaroslav O. Kvashnin,¹³ Inka L. M. Locht,^{13,33} Sven Lubeck,¹⁴ Martijn Marsman,³⁰ Nicola Marzari,⁹ Ulrike Nitzsche,³¹ Lars Nordström,¹³ Taisuke Ozaki,³⁴ Lorenzo Paulatto,³⁵ Chris J. Pickard,³⁶ Ward Poelmans,^{1,37} Matt I. J. Probert,²⁵ Keith Refson,^{38,39} Manuel Richter,^{31,32} Gian-Marcus Rignanese,¹⁹ Santanu Saha,²⁰ Matthias Scheffler,^{15,40} Martin Schlipf,²² Karlheinz Schwarz,⁵ Sangeeta Sharma,¹² Francesca Tavazza,¹⁷ Patrik Thunström,⁴¹ Alexandre Tkatchenko,^{15,42} Marc Torrent,²⁸ David Vanderbilt,²³ Michiel J. van Setten,¹⁹ Veronique Van Speybroeck,¹ John M. Wills,⁴³ Jonathan R. Yates,²⁹ Guo-Xu Zhang,⁴⁴ Stefaan Cottenier^{1,45*}



New methods
Mutual agreement



Old methods
Different values



Scorecard

0.3	0.3	0.6	1.0	0.9	0.3	1.5	0.6	0.9	0.4	1.0	0.4	0.4	6.3	13.5	1.1	2.1	0.7	1.4	
0.3		0.1	0.5	0.9	0.8	0.2	1.5	0.6	0.8	0.4	1.0	0.5	0.3	6.3	13.4	1.1	2.1	0.7	1.4
0.3	0.1		0.5	0.9	0.8	0.2	1.5	0.6	0.8	0.4	0.9	0.5	0.3	6.3	13.4	1.1	2.1	0.7	1.4
0.6	0.5	0.5		0.8	0.6	0.4	1.5	0.6	0.8	0.6	1.0	0.7	0.5	6.3	13.2	1.0	1.9	0.6	1.3
1.0	0.9	0.9	0.8		0.9	0.9	1.8	0.9	1.3	1.0	1.4	1.0	0.9	6.4	13.0	1.2	1.8	1.0	1.6
0.9	0.8	0.8	0.6	0.9		0.8	1.7	0.7	1.1	0.8	1.3	1.0	0.8	6.5	13.2	1.1	1.8	0.8	1.5
0.3	0.2	0.2	0.4	0.9	0.8		1.5	0.5	0.8	0.3	1.0	0.5	0.3	6.2	13.4	1.0	2.0	0.6	1.4

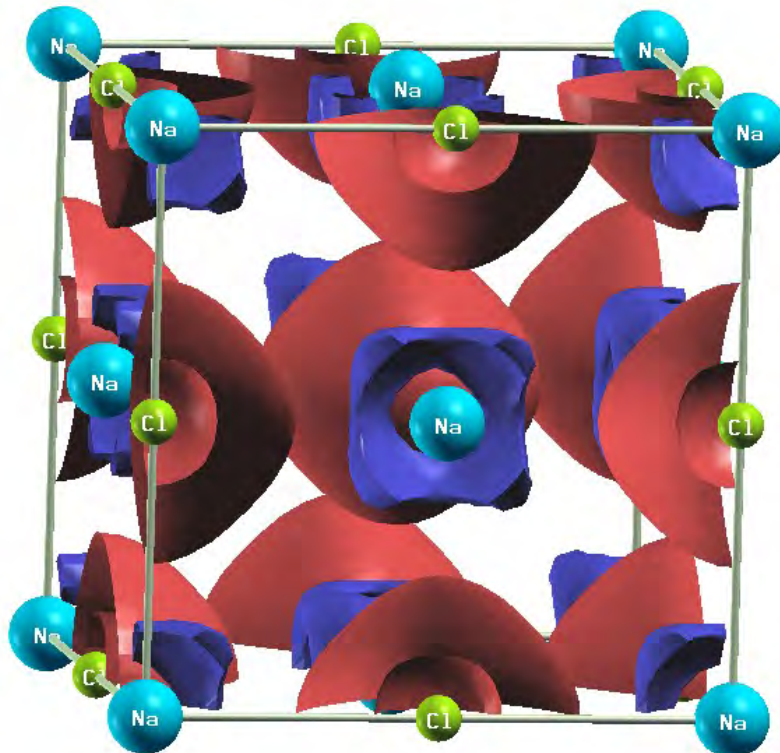
PAW vs USP accuracy

		AE								
		Elk	exciting	FHI-aims/tier2	FLUER	FPLQ/T+F+S	RSPT	WTEN2k/acc	average <Δ>	
PAW	GBRV12/ABINIT	0.9	0.8	0.8	0.9	1.3	1.1	0.8	0.9	
	GPAW09/ABINIT	1.3	1.3	1.3	1.3	1.7	1.5	1.3	1.4	
	GPAW09/GPAW	1.5	1.5	1.5	1.5	1.8	1.7	1.5	1.6	
	JTH02/ABINIT	0.6	0.6	0.6	0.6	0.9	0.7	0.5	0.6	
	PSlib100/QE	0.9	0.8	0.8	0.8	1.3	1.1	0.8	0.9	
	VASPGW2015/VASP	0.5	0.4	0.4	0.6	1.0	0.9	0.4	0.6	
USPP	GBRV14/CASTEP	1.1	1.1	1.0	1.0	1.4	1.3	1.0	1.1	
	GBRV14/QE	1.0	1.0	0.9	1.0	1.4	1.3	1.0	1.1	
	OTFG9/CASTEP	0.4	0.5	0.5	0.7	1.0	1.0	0.5	0.7	
	SSSP/QE	0.4	0.3	0.3	0.5	0.9	0.8	0.3	0.5	
	Vdb2/DACAPO	6.3	6.3	6.3	6.3	6.4	6.5	6.2	6.3	

Ionic bonding in NaCl

Charge transfer **from Na to Cl**

Unlike Si, no build up of charge between atoms



Covalent bonding in silicon

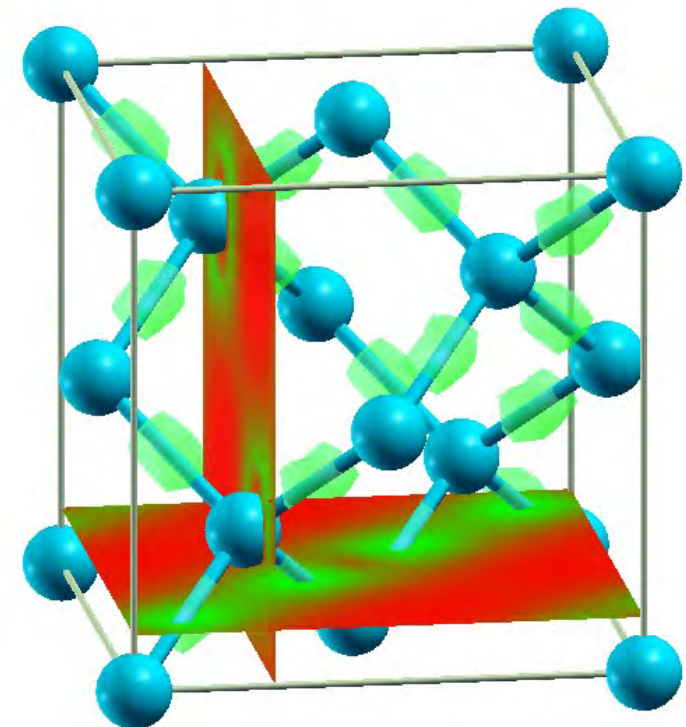
Covalent bonding arises from build up of -ve charge between +ve nuclei.

Chemical bond is **emergent property** of electron-ion system

Not merely qualitative description – can compute bond and cohesive energy.

($E_{coh} = 5.45 \text{ eV}$; expt 4.62 eV)

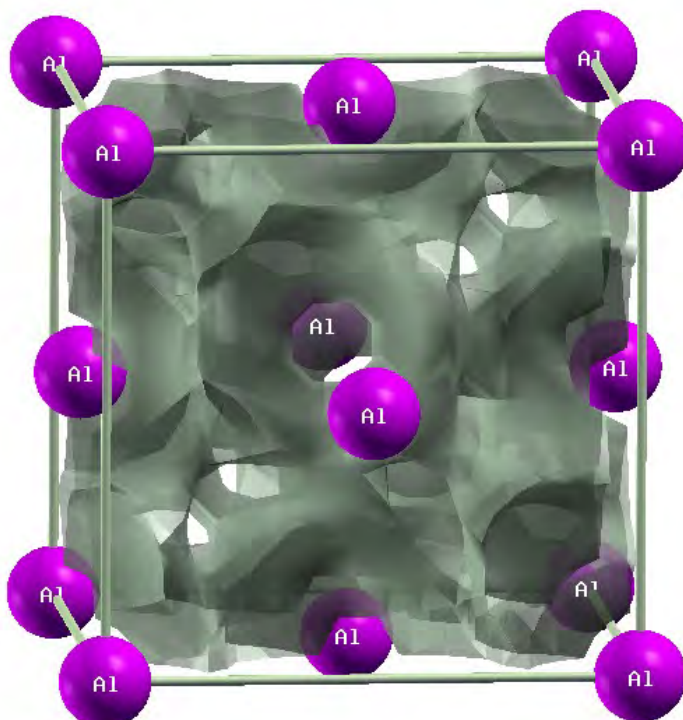
Lattice Parameter $a_0 = 0.549\text{nm}$ (0.5431nm)



Metallic bonding in aluminium

Valence electrons are spread out – metallic state.

Calculation shows no **band gap**; correctly predicts Al is **metallic**.



No van Der Waals Bonding

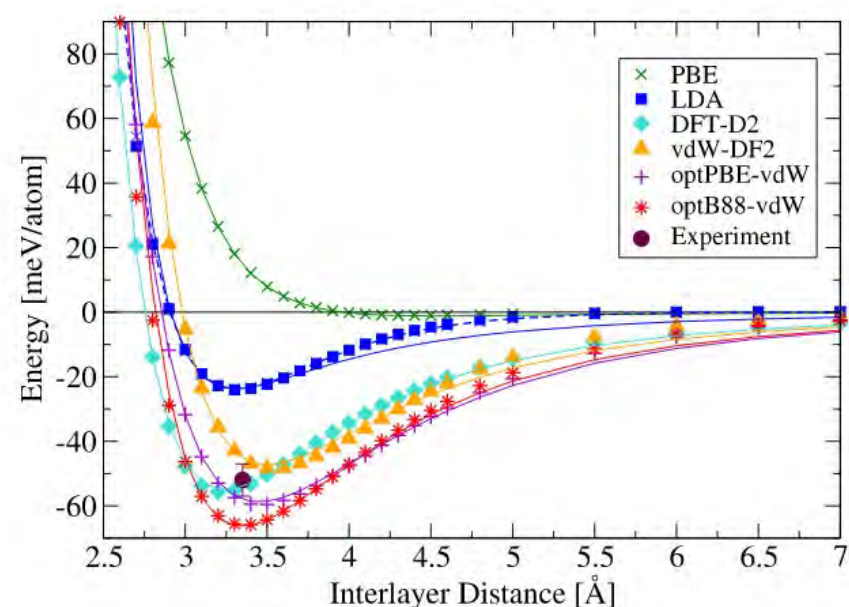
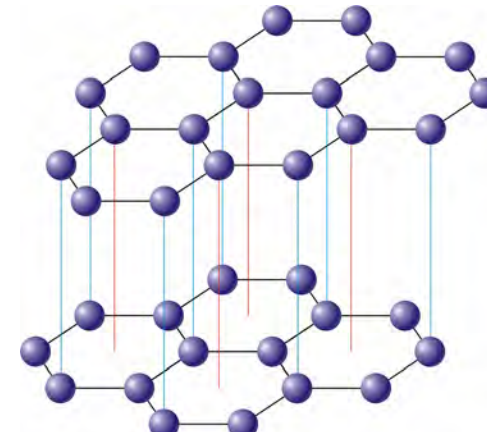
LDA, GGA, m-GGA and hybrids **do not** include non-bonded van-der Waals interactions.

3

Example: Graphite

Non-polar molecular crystals can be completely unbound!

A variety of semi-empirical correction schemes exist to add missing interaction.



Electronic Spectra

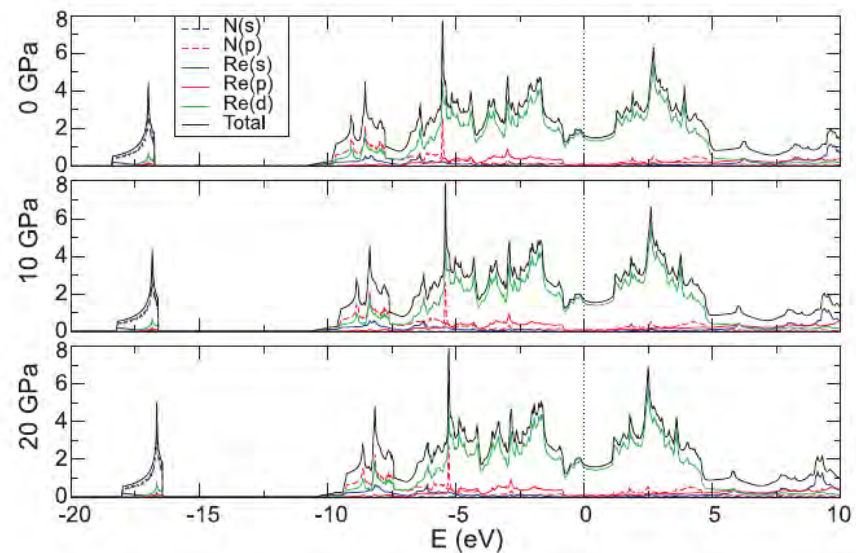
Strictly, DFT has no basis to describe excited states. However unoccupied K-S states do resemble single-electron excitations. It is predictive for some spectroscopies, ignoring band-gap error:

- UV-Vis (but not excitons)
- EELS and Xanes

But some excitations have no K-S counterpart.

- Magnons
- Excitons

and a higher level of theory treatment is required. (eg Bethe-Salpeter)

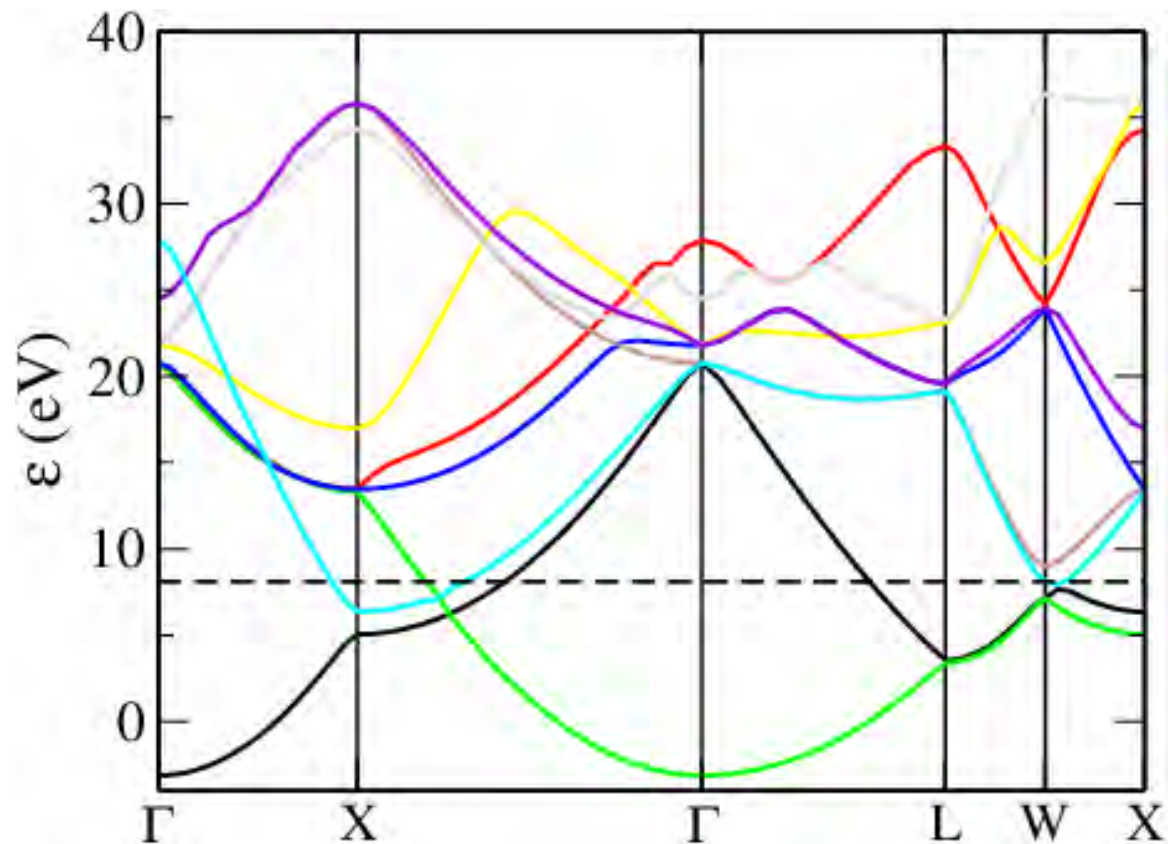




From bands to properties

Band-theory perspective

$$\hat{H} \Psi_i = \epsilon_i \Psi_i$$



1980s: Total Energy Calculations

$$E_{tot} = \langle \Psi | \hat{H} | \Psi \rangle = E_{BS} + E_{I-I} - E_{e-e}$$

Total energy calculations in solid state physics

J Ihm†

Bell Communications Research, Murray Hill, New Jersey 07974, USA

Abstract

Total energy calculations for the study of atomic and electronic structures of solids are reviewed. A history of total energy calculations in solid state physics from the emergence of quantum physics to the mid 1970s is briefly summarised. Important developments in the last decade, the period during which computing capability has grown explosively all over the world, are then described. Modern computational method are discussed in detail, with emphasis on the tight-binding, quantum-chemical

Totally Useless?

$$E_{tot} = E_{BS} + E_{I-I} - E_{e-e}$$

Totally Useless?

$$E_{tot} = E_{BS} + E_{I-I} - E_{e-e}$$

$$P = -\frac{dE_{tot}}{dV}$$

$$F_j = -\frac{dE_{tot}}{dR_j}$$

$$\Phi_{i,j} = \frac{d^2 E_{tot}}{dR_i dR_j}$$

$$\alpha_{ij} = \frac{d^2 E_{tot}}{dE_i dE_j}$$

Totally Useless?

$$E_{tot} = E_{BS} + E_{I-I} - E_{e-e}$$

$$P = -\frac{dE_{tot}}{dV}$$

$$F_j = -\frac{dE_{tot}}{d} R_j$$

$$\Phi_{i,j} = \frac{d^2 E_{tot}}{d R_i d R_j}$$

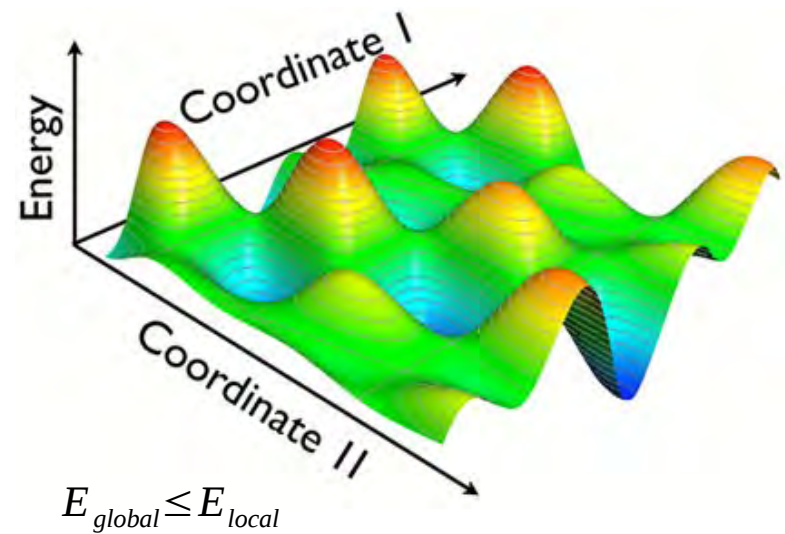
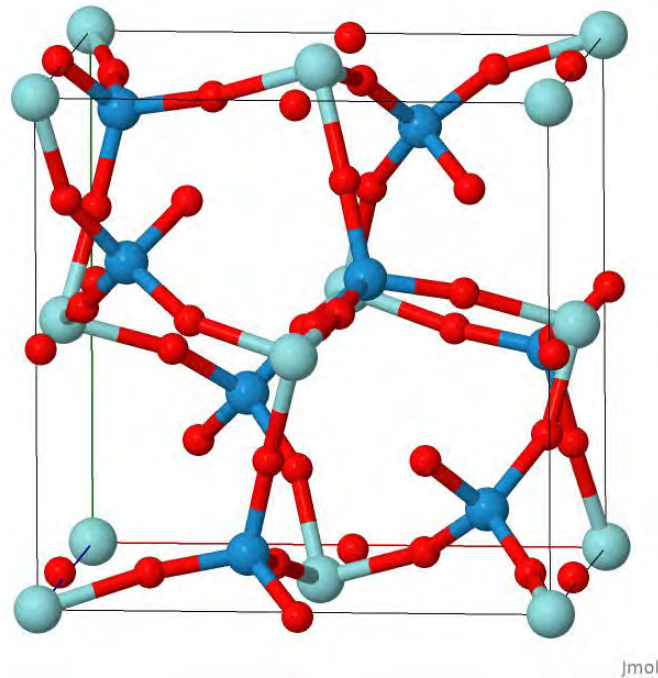
$$\alpha_{ij} = \frac{d^2 E_{tot}}{d E_i d E_j}$$

$$I_{m,i,j}^{raman} \propto \frac{d^3 E_{tot}}{d E_i d E_j d Q_m}$$

$$\chi_{i,j,k}^{(2)} \propto \frac{d^3 E_{tot}}{d E_i d E_j d E_j}$$

$$\frac{\delta \omega}{\omega} \sim \frac{d^3 E_{tot}}{d R_i d R_j d R_k}$$

The Optimization Problem



$$E(x_1, y_1, z_1, \dots) \leq E_0$$

iterative downhill optimization methods can find local minima

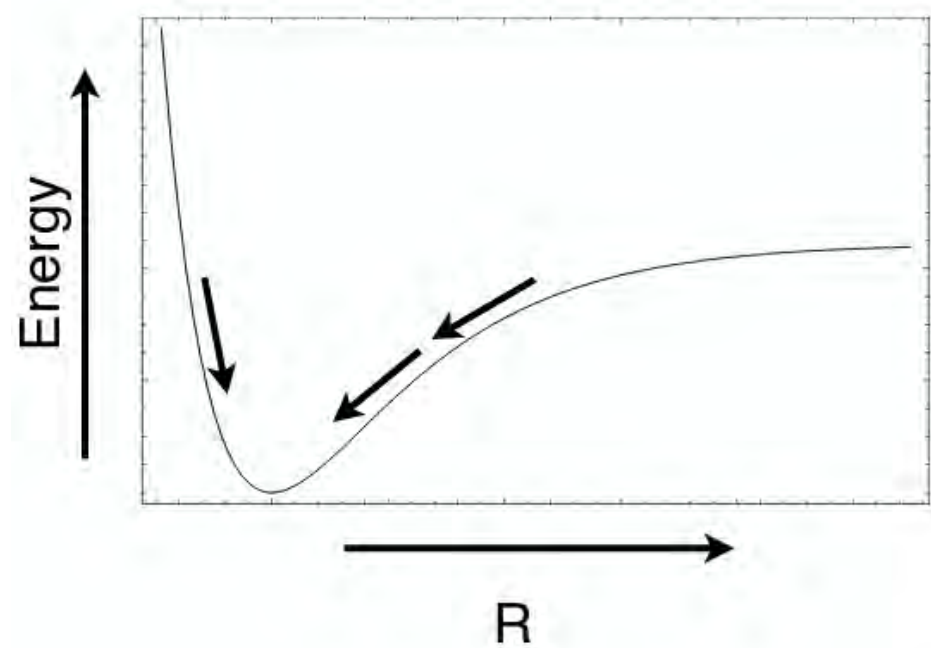
Forces and Geometry

The Hellman-Feynman Theorem gives forces if ground state known

$$F_i = -\langle \Psi_0 | \frac{d E}{d x_i} | \Psi_0 \rangle$$

Can move atoms in response to computed forces.

Apply machinery of optimization theory:
E.g. quasi-Newton methods (BFGS) to find equilibrium crystal structure.



DFT Simulation Codes

Planewave

CASTEP PEtot
VASP PARATEC
PWscf Da Capo
Abinit CPMD
Qbox fhi98md
PWPAW SFHIngX
DOD-pw NWchem
Octopus JDFTx

Gaussian

CRYSTAL
CP2K
AIMPRO

Numerical

FHI-Aims
SIESTA
Dmol
ADF-band
OpenMX
GPAW
PARSEC

DFT

$\Psi(r)$, $n(r)$

LMTO

LMTART
LMTO
FPLO

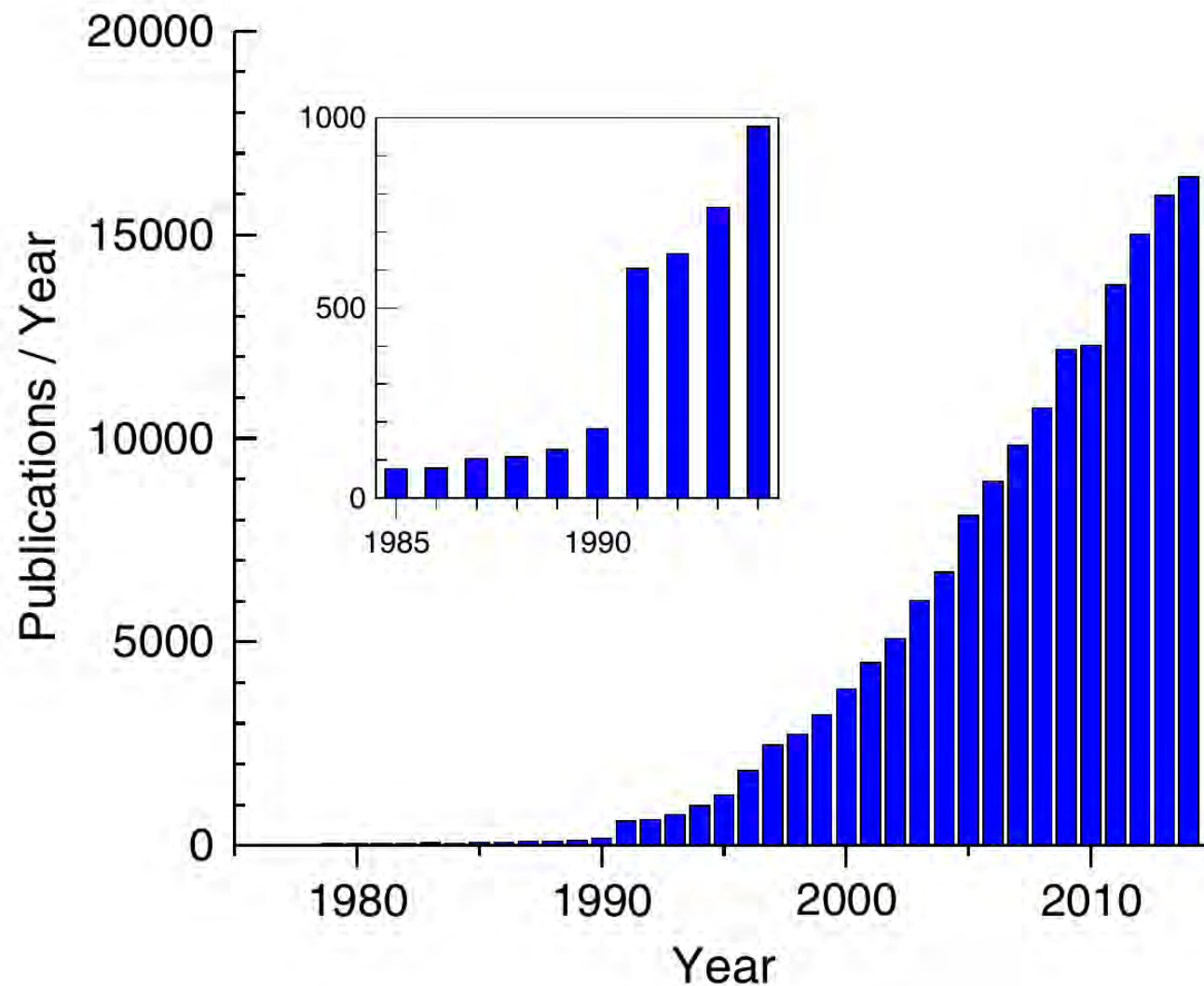
$O(N)$

ONETEP
Conquest
BigDFT

LAPW

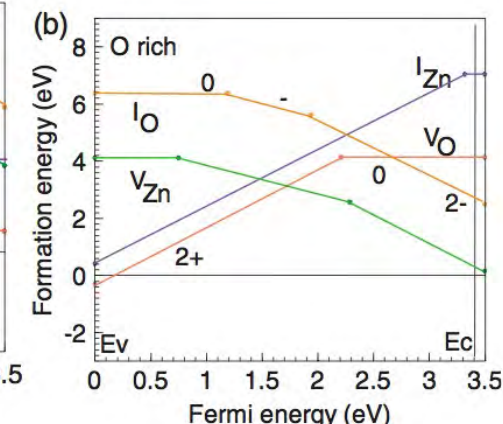
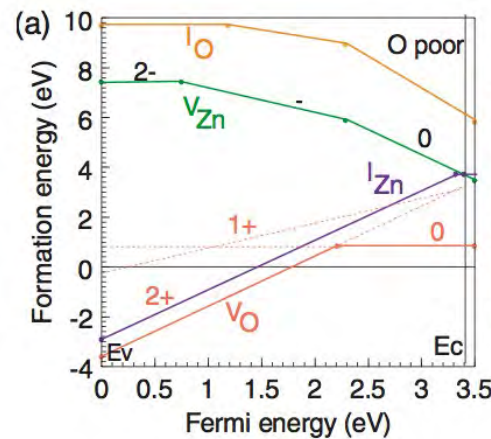
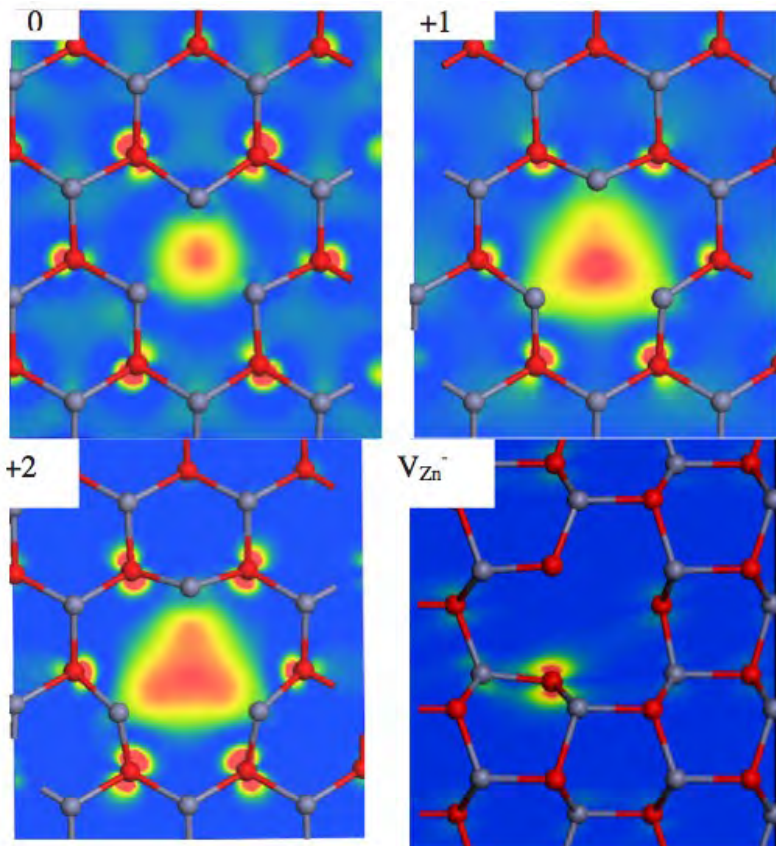
WIEN2k
Fleur
exciting
Elk

Popularity of DFT



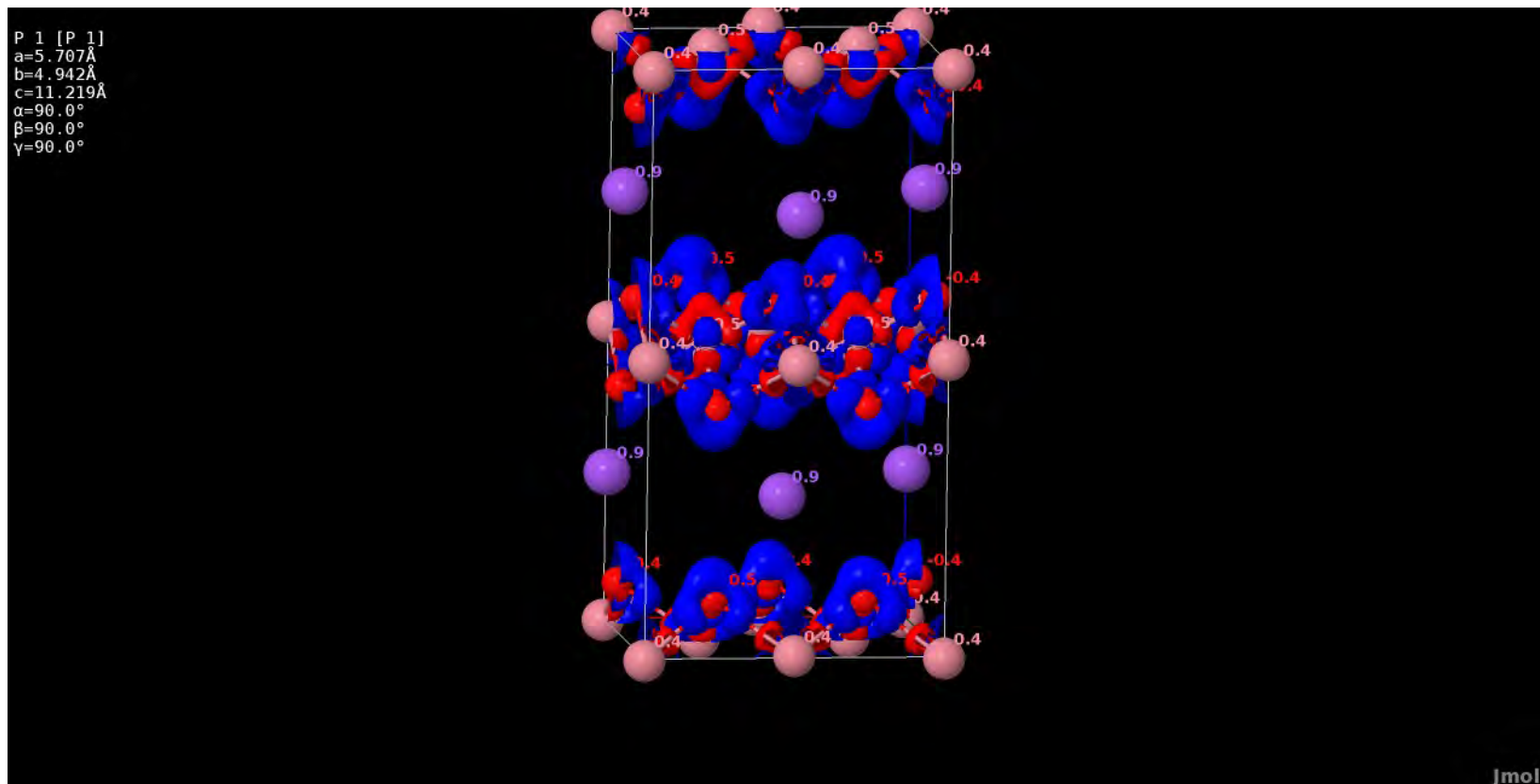
Electronic Structure

Charged Defects in ZnO



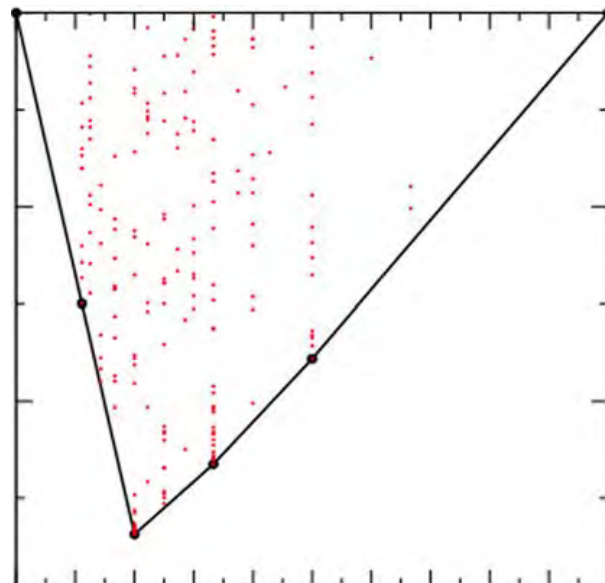
-
-
-
-

Charge ordering (with DFT+U)

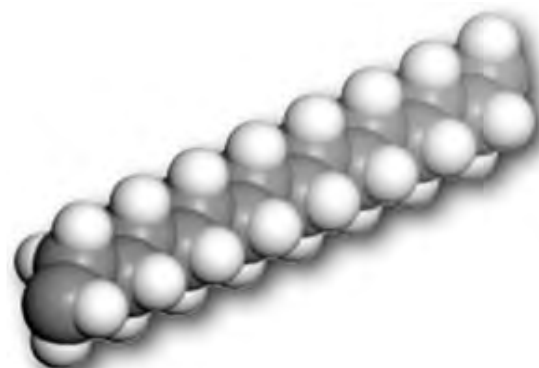
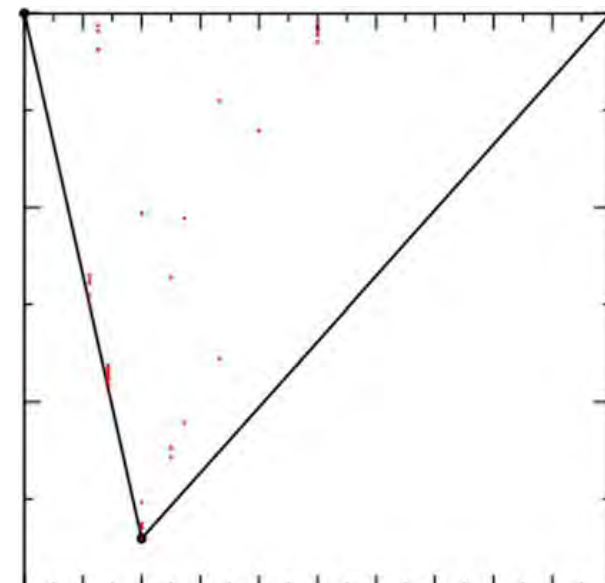


Crystal Structure

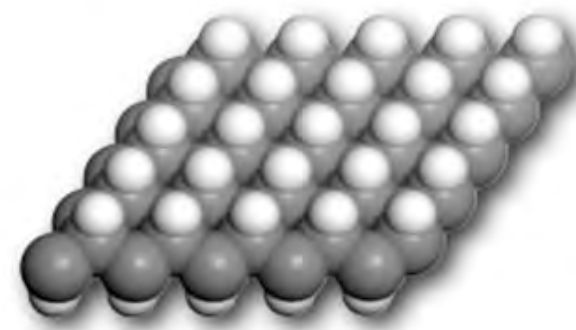
AIRSS: Prediction of Crystal Structures



methane

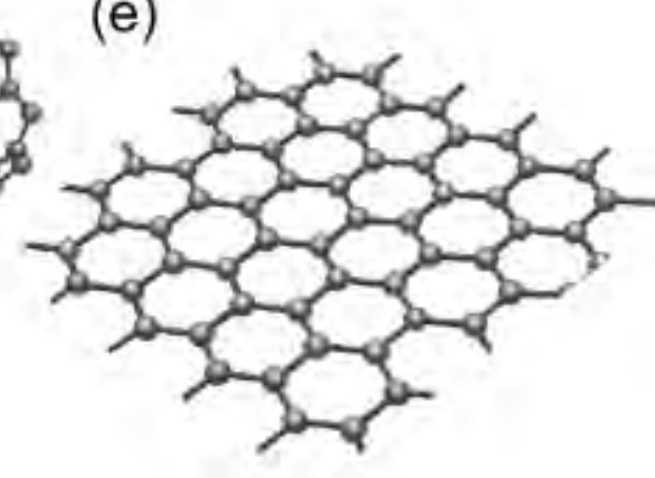
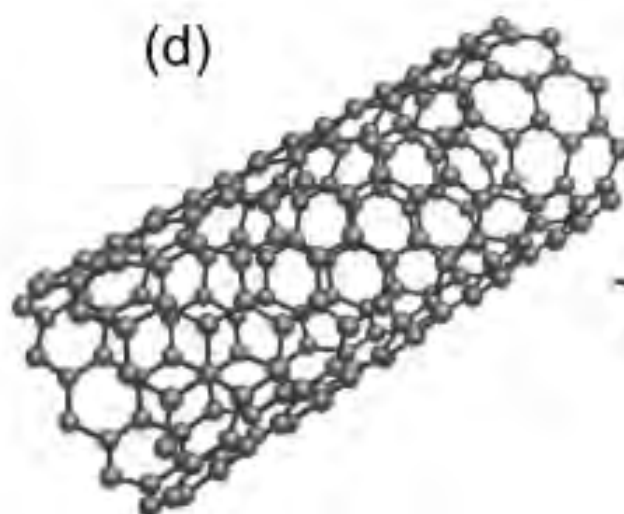
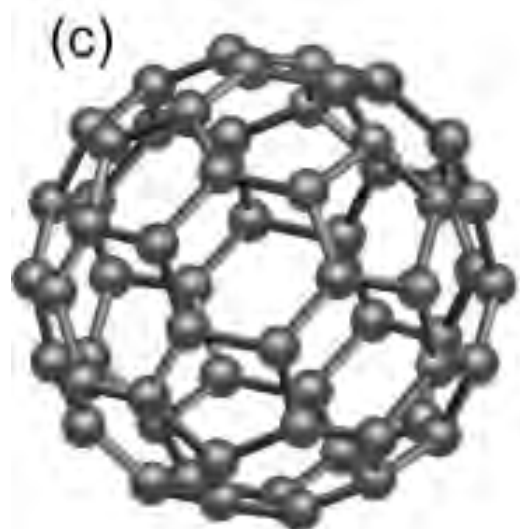
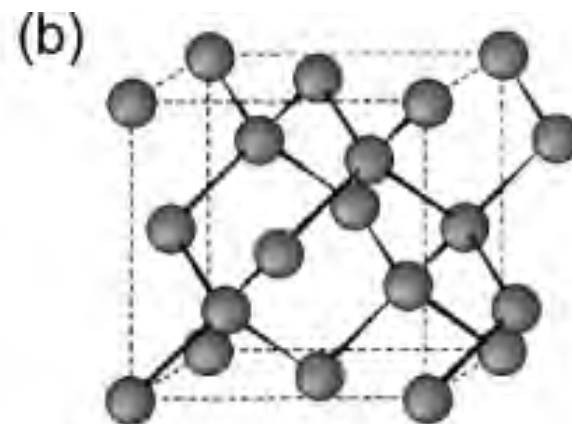
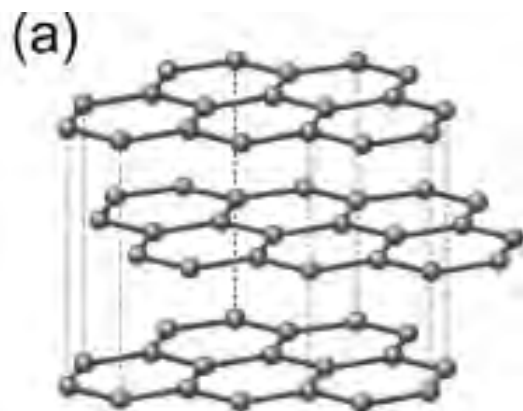


polyethane



graphane

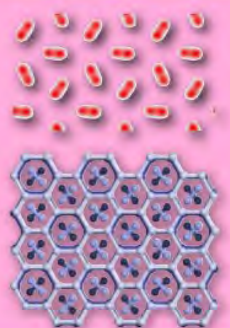
Predicting Structure



AIRSS - A tool for discovery

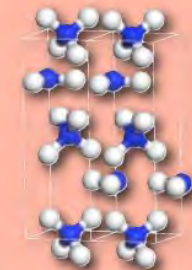
**Hydrogen is
polar and
“graphene”**

Nature Physics, 2007
Physical Review B, 2012



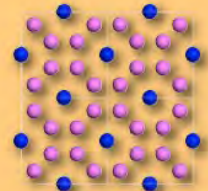
Ammonia is ionic

Nature Materials, 2008



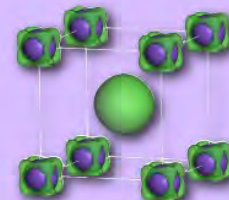
**Aluminium is
complicated**

Nature Materials, 2010



**Magnetic
potassium**

Physical Review Letters, 2011



Molecular Dynamics

Dynamics of nuclei

With forces calculated from DFT

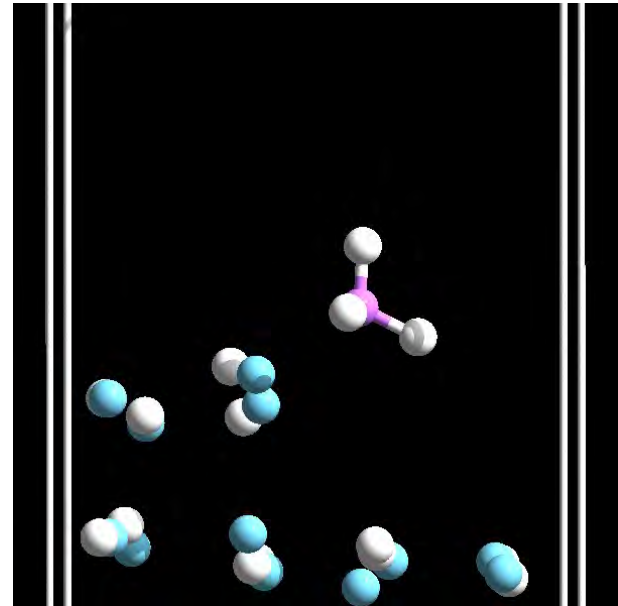
Can also calculate **dynamics**:

- Molecular dynamics – time evolution
- Lattice dynamics - spectroscopy

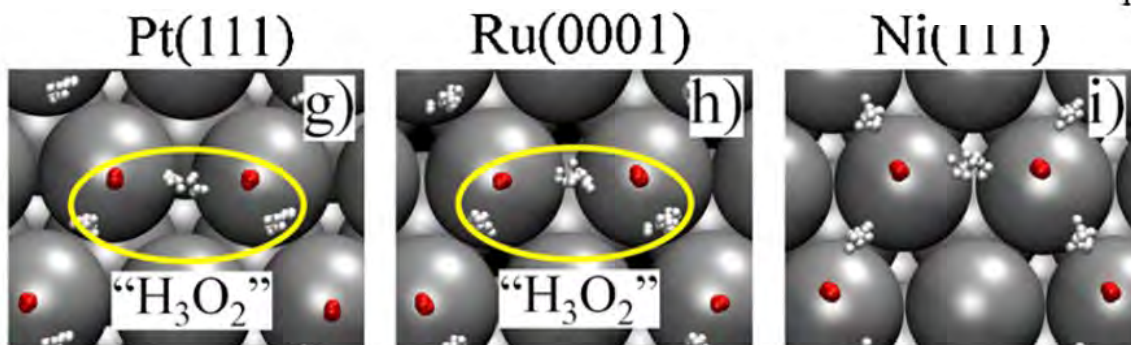
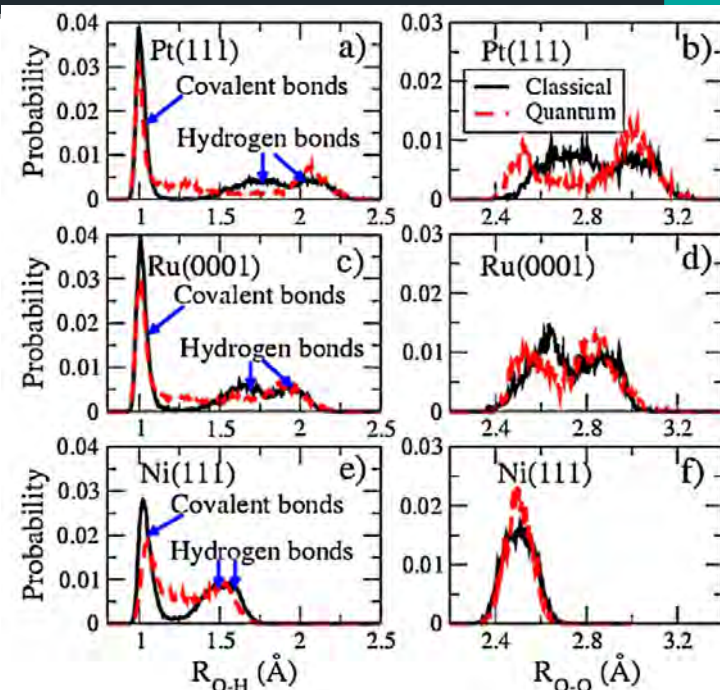
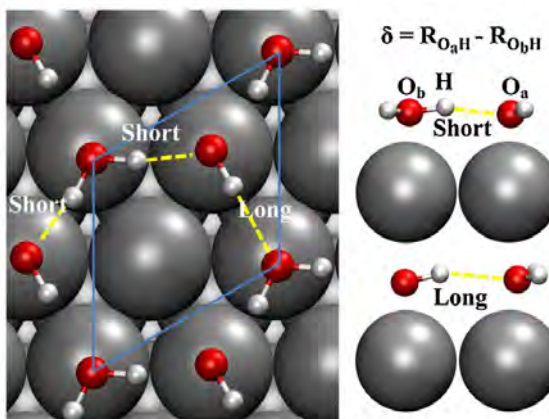
$$r(t+\delta t) = r(t) + v(t)\delta t + \frac{1}{2}a(t)\delta t^2$$

$$v(t+\delta t) = v(t) + \frac{1}{2}[a(t) + a(t+\delta t)]\delta t$$

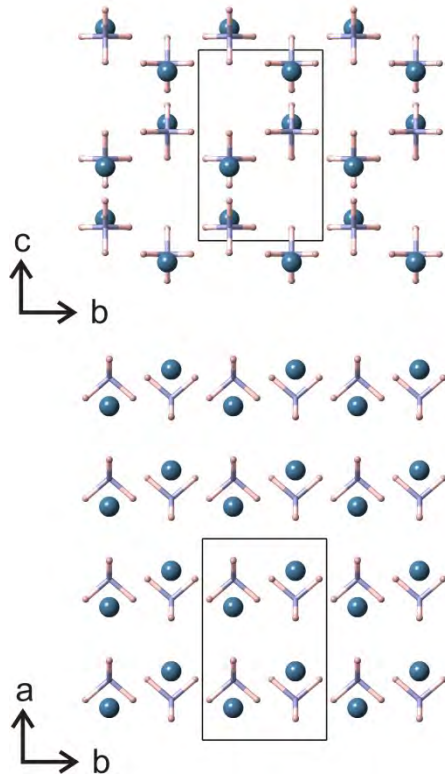
$$a(t+\delta t) = \frac{1}{m} F(t+\delta t)$$



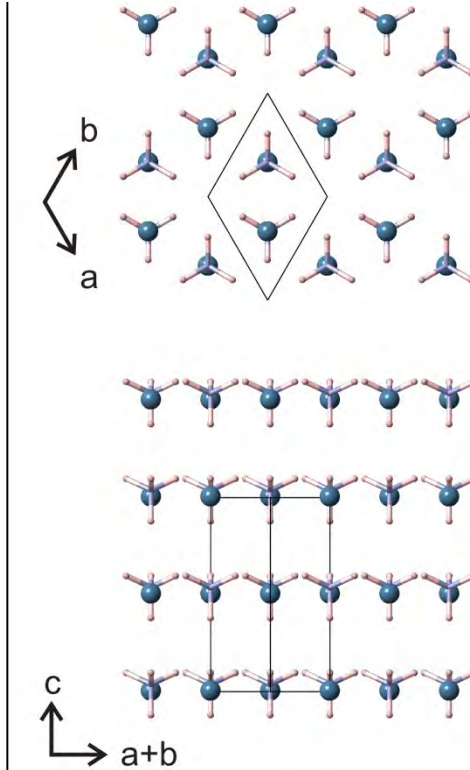
Water on metal Surfaces



Fast-ion conduction in LiBH_4



< 390 K
Orthorhombic (Pnma)



> 390 K
Hexagonal (P63/mmc)
Disordered
Superionic conductivity

> 560 K: liquid
> 650 K: decomposition

A little knowledge?

unsuccessful attempts to model high-temperature phase by optimisation and lattice dynamics:

- Miwa, K. et al., 2004. First-principles study on lithium borohydride LiBH₄. Physical Review B, 69(24), 245120.

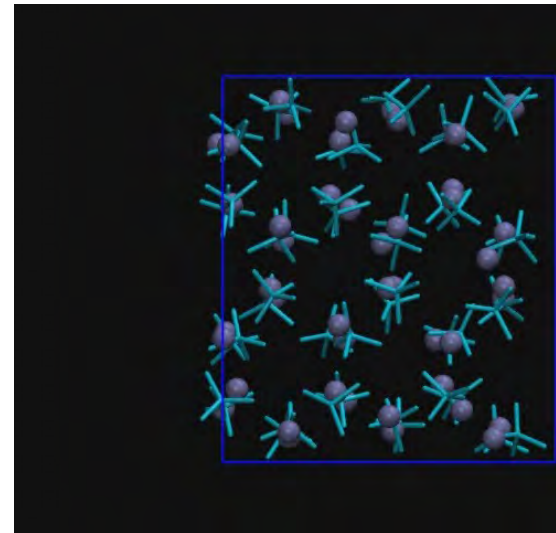
"The finite temperature effects are probably crucial to study the structural properties in this phase."
- Tekin, A. et al., 2010. First-Principles Determination of the Ground-State Structure of LiBH₄. PRL, 104(21), p.215501.
- Łodziana, Z. & Vegge, T., 2004. Structural Stability of Complex Hydrides: LiBH₄ Revisited. PRL, 93(14), p.145501.

"At finite temperatures a stable crystalline structure requires all phonon frequencies to be positive definite: $\omega^2 > 0$ a significant part of the phonon spectrum for the P63mc phase is imaginary—which means that this structure is unstable at T>0K. This surprising result, considering the experimental predictions ... "
- Łodziana, Z. & Vegge, T., 2006. Łodziana and Vegge Reply: Physical Review Letters, 97(11), p.119602.

"A system which is unstable within the harmonic approach can be stabilized by entropy, in which case it must posses more than dynamical disorder."

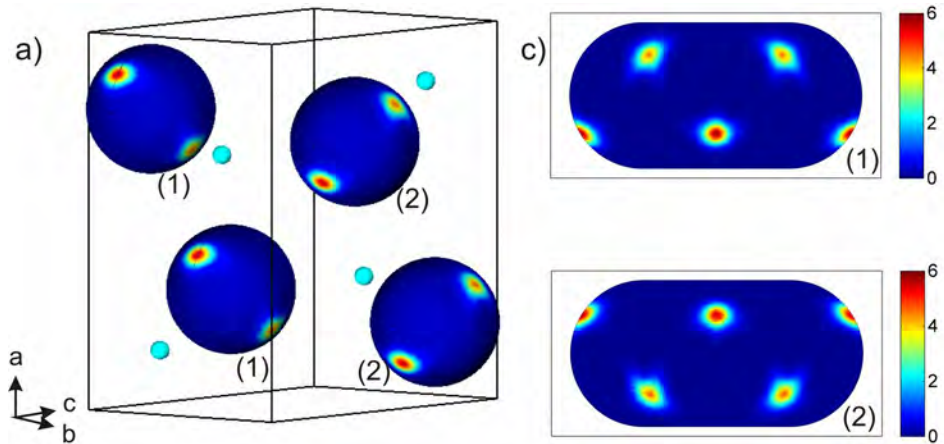
AIMD – computational details

- Code: CP2K (out-of-the-box)
- Born-Oppenheimer molecular dynamics in isokinetic ensemble (Gaussian thermostat)
- Forces evaluated by DFT using the QUICKSTEP method
- Supercell: 288 atoms (48 formula units)
- Time step: 0.5 fs
- Run lengths 20-30 ps after equilibration
- PBE exchange-correlation functional
- Dual basis set (Gaussian DZ orbitals & plane waves up to 280 Ry) and Goedecker pseudopotentials are used

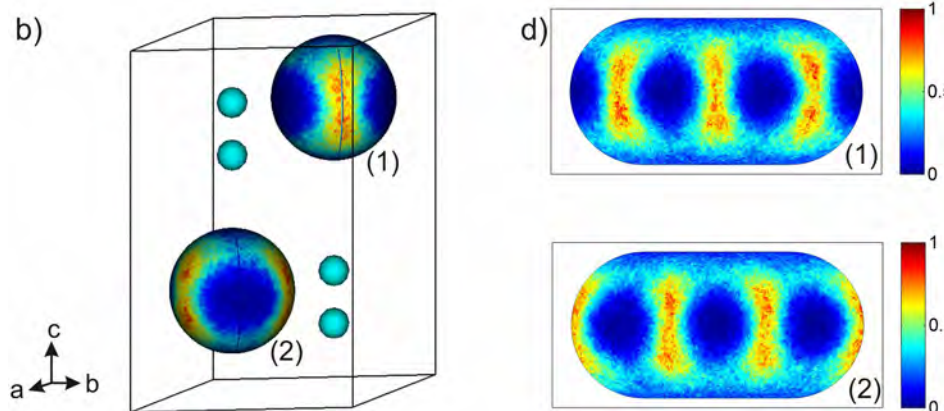


Equilibrium MD picture

BH4 rotational disorder:



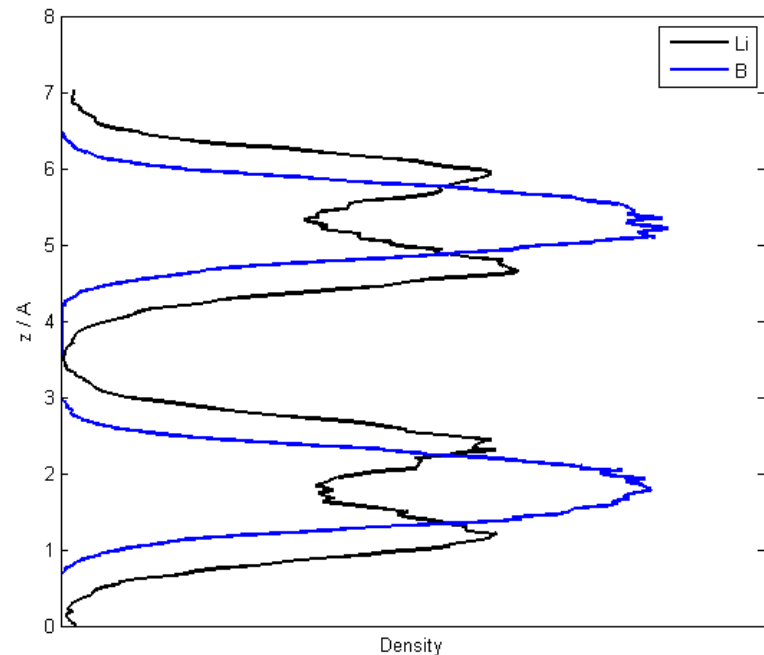
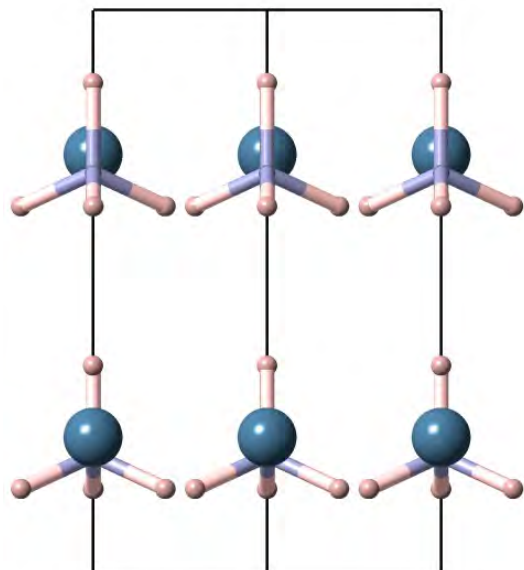
298K



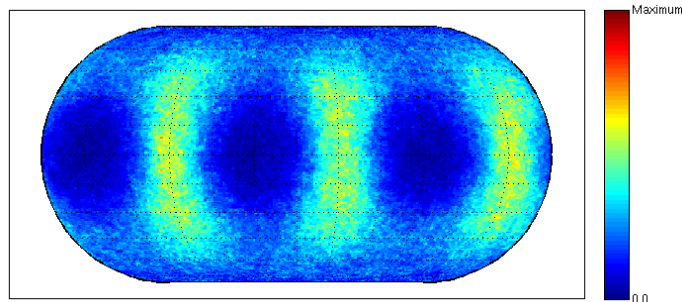
473K

Equilibrium MD picture

Li dynamical disorder:



BH₄ rotational disorder:



The Nature of BH_4^- Reorientations in Hexagonal LiBH_4

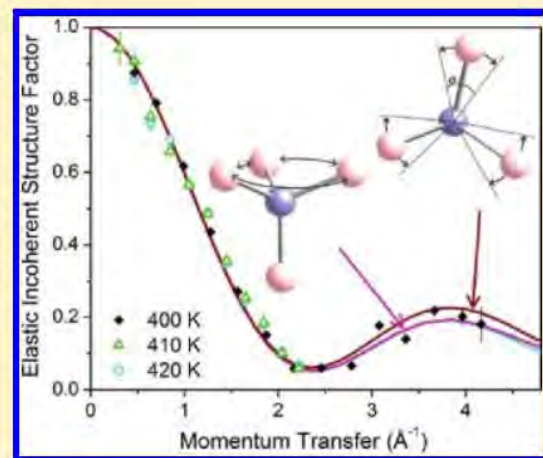
Nina Verdal,^{*,†} Terrence J. Udovic,[†] and John J. Rush^{†,‡}

[†]NIST Center for Neutron Research, National Institute of Standards and Technology, 100 Bureau Dr., MS 6102, Gaithersburg, Maryland 20899-6102, United States

[‡]Department of Materials Science and Engineering, University of Maryland, 2135 Chemical & Nuclear Engineering Bldg., College Park, Maryland 20742-2115, United States

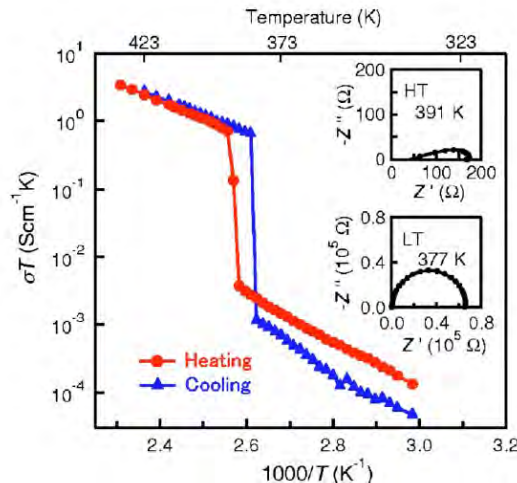
 Supporting Information

ABSTRACT: Lithium borohydride (LiBH_4) has lately been the subject of intense inquiry within the hydrogen storage community. Quasi-elastic neutron scattering spectra were measured for LiBH_4 in the high-temperature hexagonal crystal phase. The elastic incoherent structure factor associated with the rapid BH_4^- anion reorientations was determined at 400, 410, and 420 K for momentum transfers as high as 4.2 \AA^{-1} . The results strongly suggest a BH_4^- reorientational mechanism approaching quasi-free, trigonal-axis rotation of three borohydride H atoms, combined with reorientational jump exchanges between these delocalized “orbiting” H atoms and the remaining axial borohydride H atom. This mechanism is consistent with previously reported diffraction and spectroscopy studies.

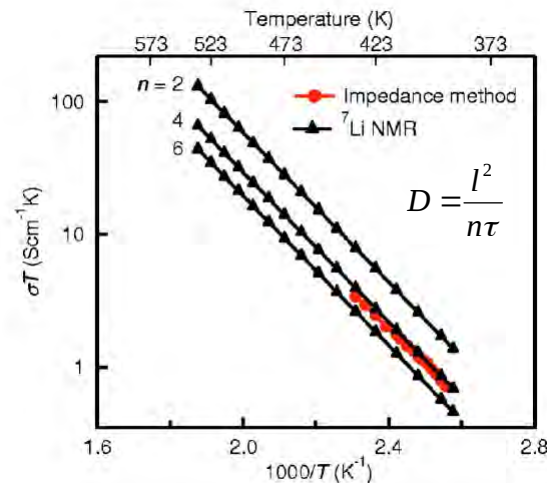


Measurements of Li mobility

Motoaki Matsuo et al., Applied Physics Letters **91**, 224103 (2007).



A/C impedance measurements



Li-7 NMR measurements

At 535K:

$$\sigma = 0.139 \text{ S/cm}$$

$$D_{\text{Li}} = 2.28 \cdot 10^{-6} \text{ cm}^2/\text{s}$$

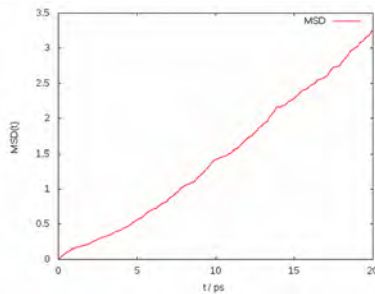
Calculating diffusion by AIMD

Diffusion coefficient calculated by...

Einstein-Sutherland equation

$$D = \frac{1}{n} \frac{d\langle r^2(t) \rangle}{dt}$$

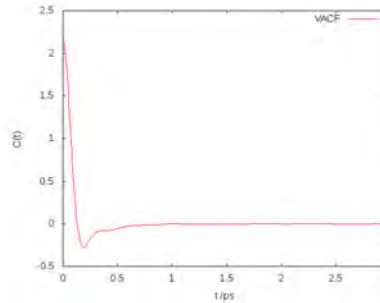
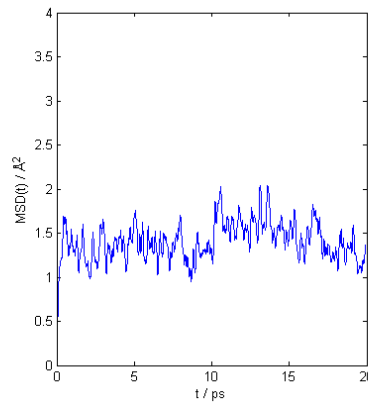
Lennard-Jonesium
(mimicking liquid Argon)



Green-Kubo formula

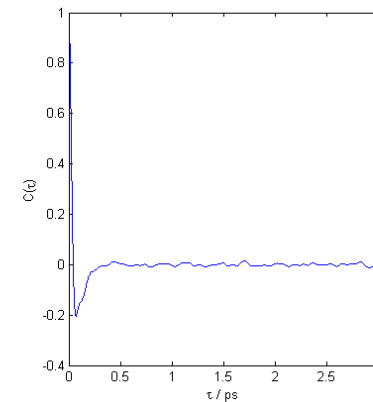
$$D = \frac{2}{n} \int_0^\infty dt \langle v(0) \cdot v(t) \rangle$$

LiBH₄ at 535 K



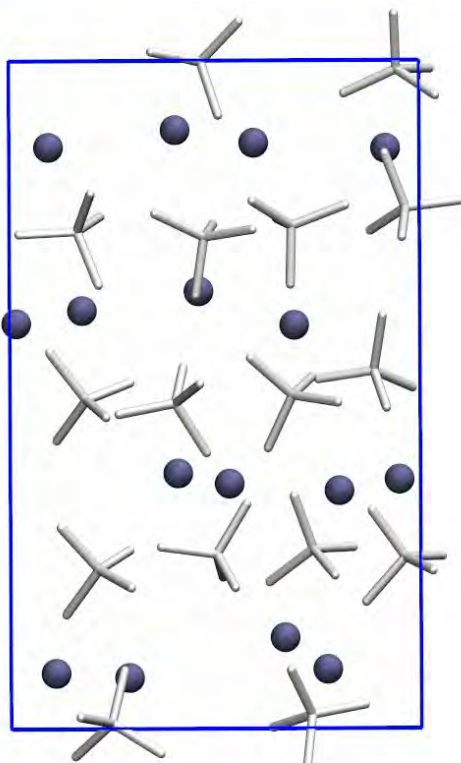
Fast diffusion

Diffusion by ion jumps
(rare events)
which are often
followed by a jump back
to the original position



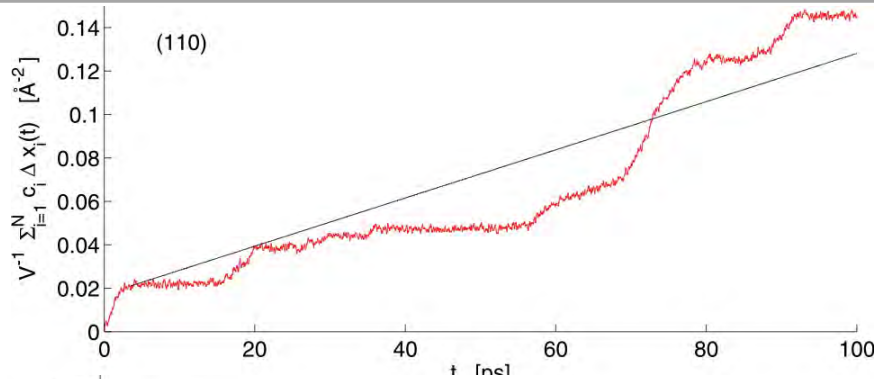
Limits of AIMD: diffusion in fluids with $D > 10^{-5} \text{ cm}^2/\text{s}$

Nonequilibrium Molecular Dynamics

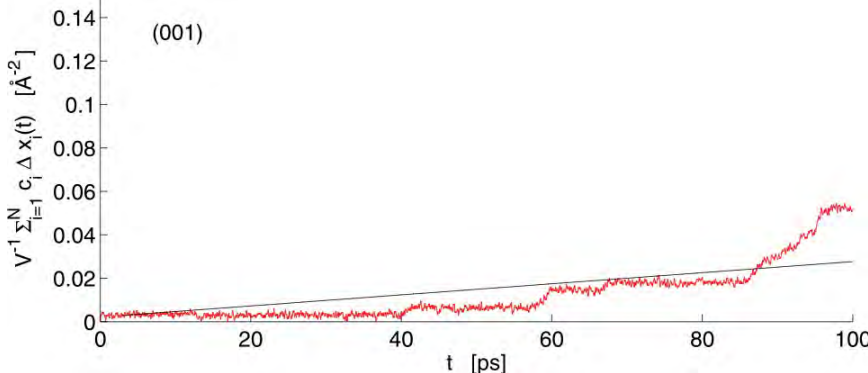


- An external field \mathbf{F}_e is applied that couples to a fictitious atomic property (“colour”, c_i):
$$\dot{\mathbf{p}}_i = \mathbf{F}_i + c_i \mathbf{F}_e$$
- The (fictitious) field and its induced response are related by (real) transport coefficients:
$$D = \frac{k_B T}{\rho_c} \lim_{t \rightarrow \infty} \lim_{F_e \rightarrow 0} \frac{\langle J_c(t) \rangle}{F_e}$$
- NEMD functionality implemented in CASTEP and CP2K
- *ab initio* nature of the method allows mechanism discovery

Results – $F_e = 0.05 \text{ eV}/\text{\AA}$

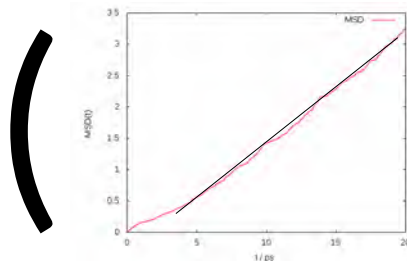


$$D_{\text{Li}} = 5.82 \cdot 10^{-6} \text{ cm}^2/\text{s}$$



$$D_{\text{Li}} = 1.34 \cdot 10^{-6} \text{ cm}^2/\text{s}$$

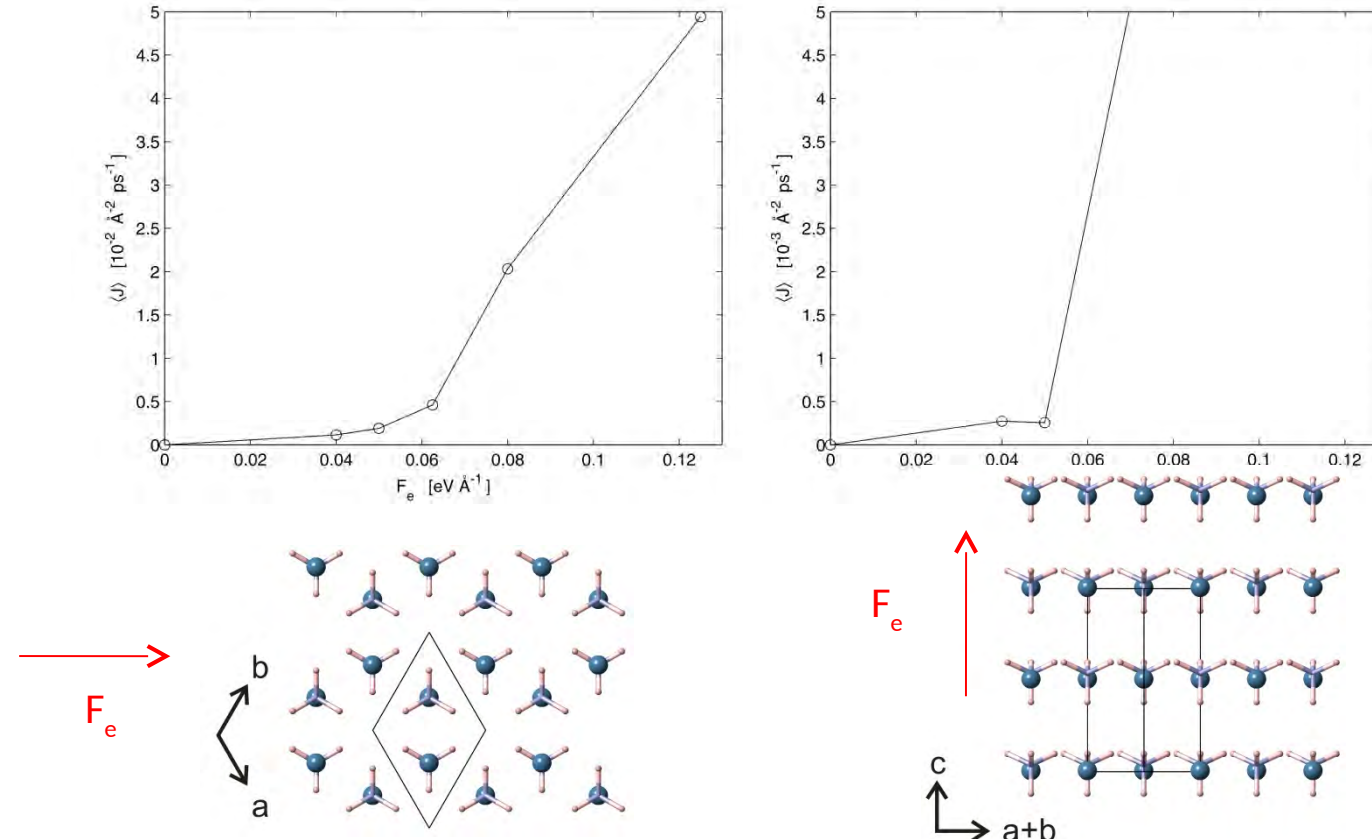
(Measured: $D_{\text{Li}} = 2.28 \cdot 10^{-6} \text{ cm}^2/\text{s}$)



Compare: $D = \frac{1}{n} \frac{d\langle r^2(t) \rangle}{dt}$

$$vs \quad D = \frac{k_B T}{\rho_c} \lim_{t \rightarrow \infty} \lim_{F_e \rightarrow 0} \frac{\langle J_c(t) \rangle}{F_e}$$

linear response domain



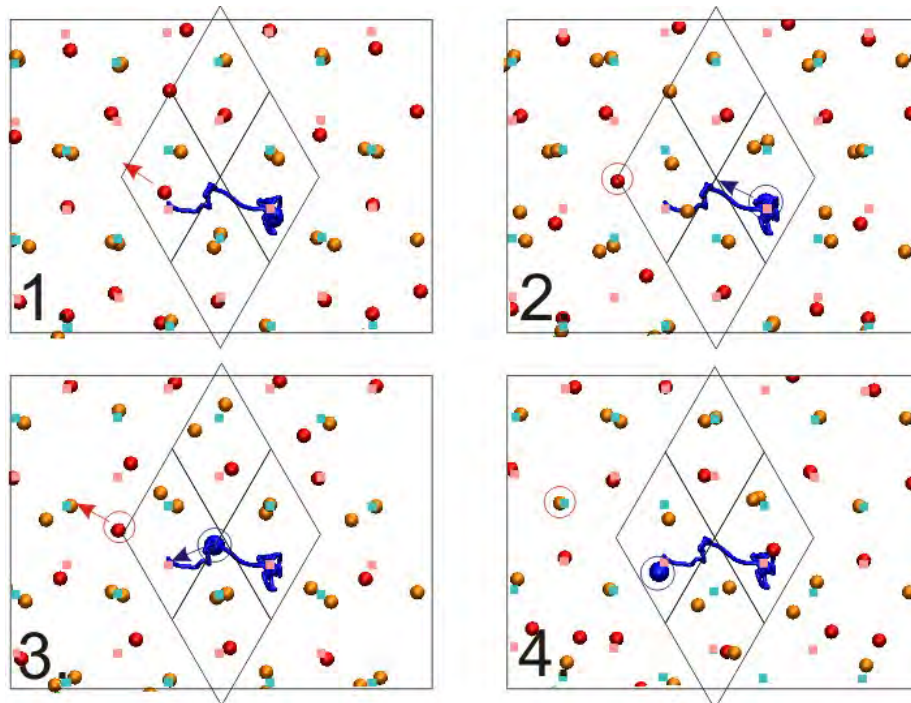
Maximum field strength in linear regime: 0.05 eV/Å

$$D(110)/(001) = 5.8 \times 10^{-6} / 1.3 \times 10^{-6} \text{ cm}^2 \text{s}^{-1}$$

$$D(\text{expt, avg.}) = 2.3 \times 10^{-6} \text{ cm}^2 \text{s}^{-1}$$

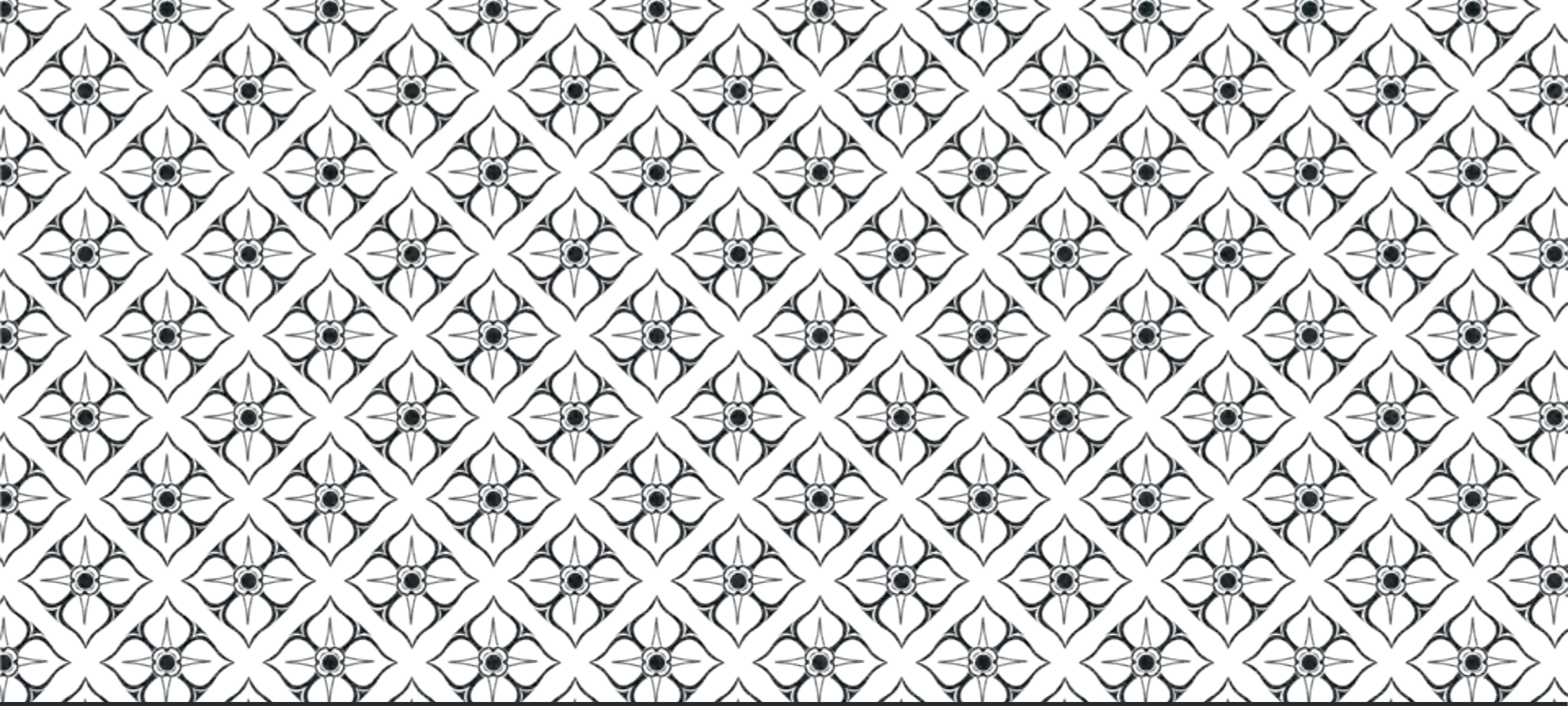
Diffusion Pathway

Inspection of the NEMD trajectory:

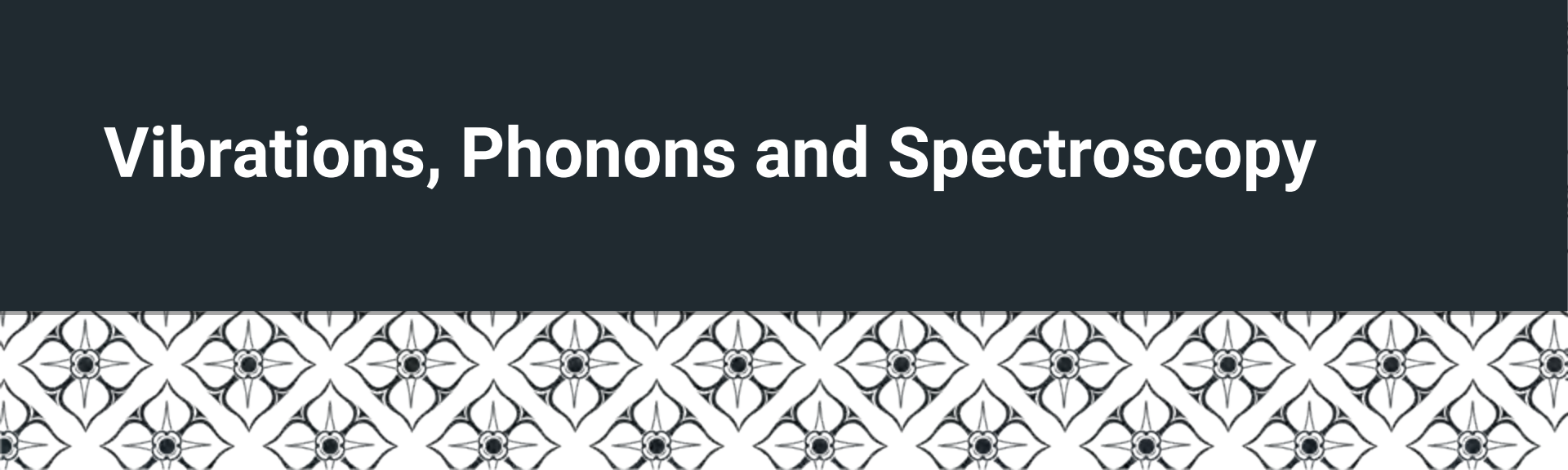


hopping is via jumps from a lattice site into an empty interstitial site (2 & 3),
and from there on to another lattice site (4).

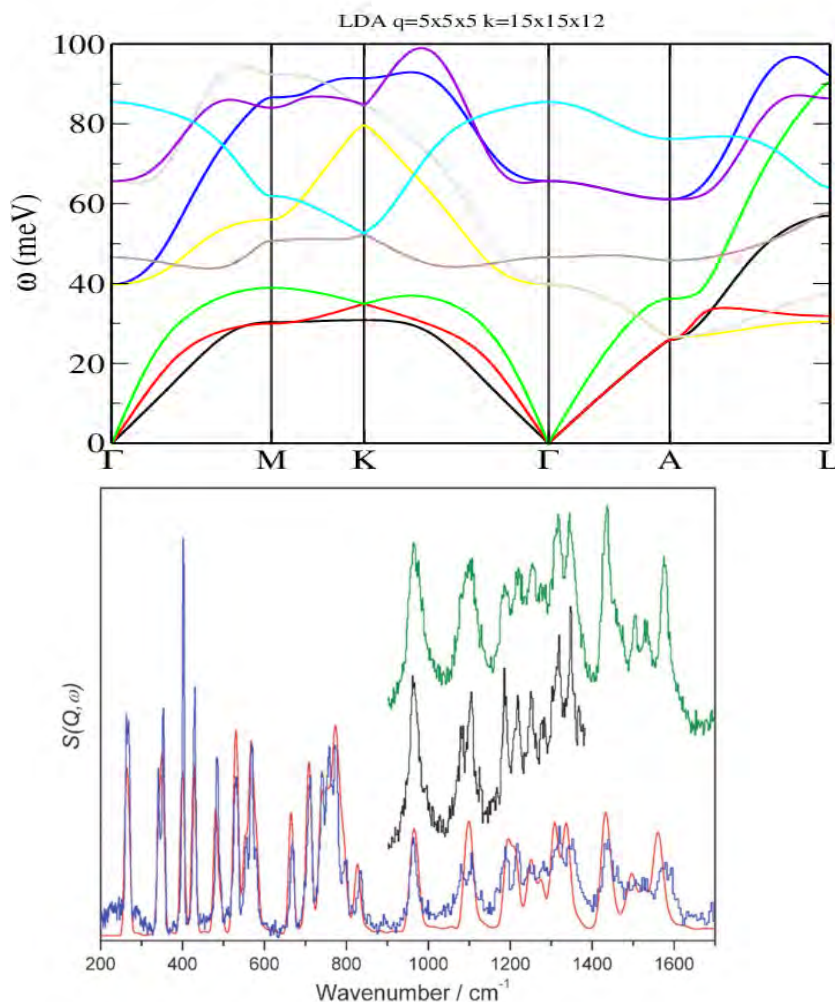
P.C. Aeberhard, S. Williams, D. Evans, K. Refson, and W.I.F. David, Physical Review Letters 108, 095901 (2012).



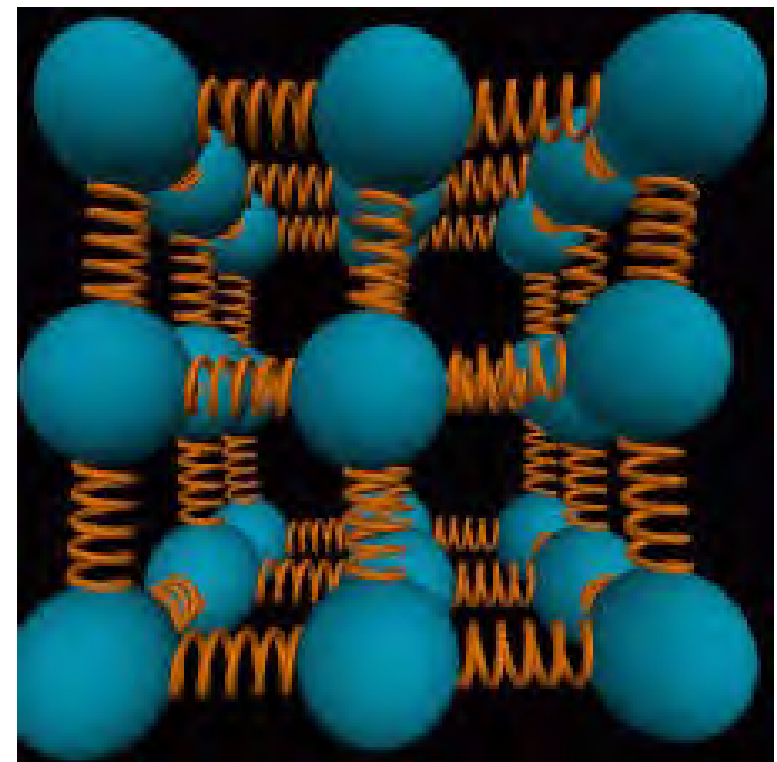
Vibrations, Phonons and Spectroscopy



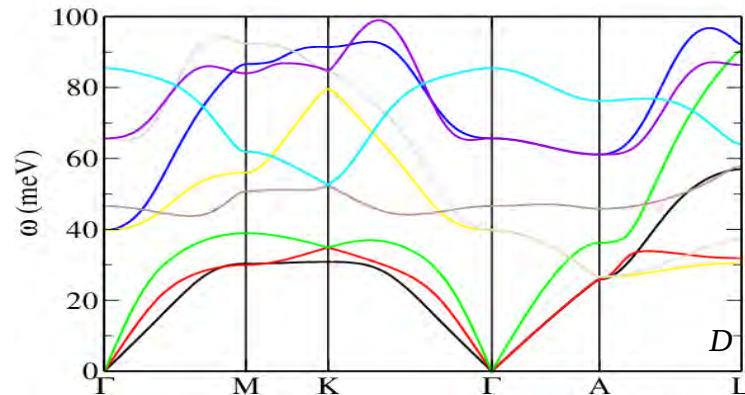
Vibrational Spectroscopy



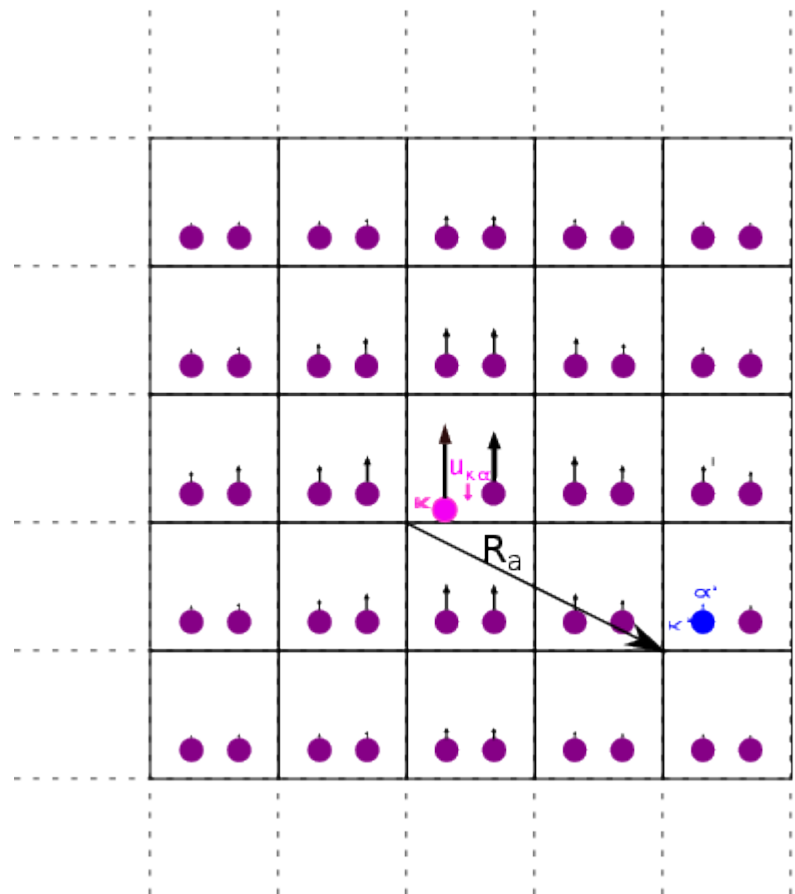
$$\Phi_{\kappa' \alpha'}^{\kappa \alpha}(\mathbf{0}, \mathbf{R}) = \frac{\partial^2 E}{\partial r_{\kappa \alpha} \partial r_{\kappa' \alpha'}}$$



Vibrational Spectroscopy



$$\Phi_{\kappa' \alpha'}^{\kappa \alpha}(\mathbf{0}, \mathbf{R}) = \frac{\partial^2 E}{\partial r_{\kappa \alpha} \partial r_{\kappa' \alpha'}}$$

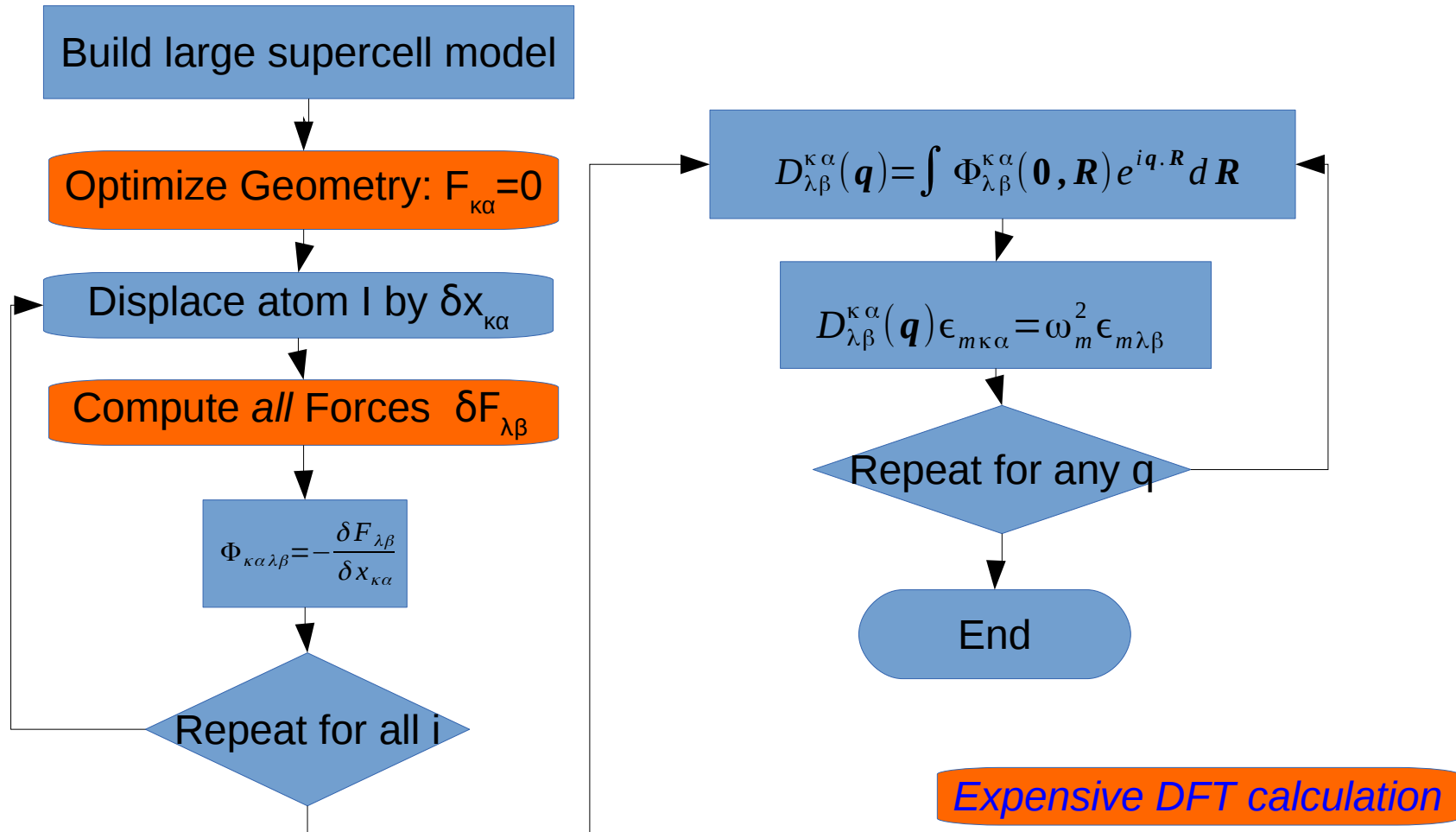


Lattice dynamics from first principles

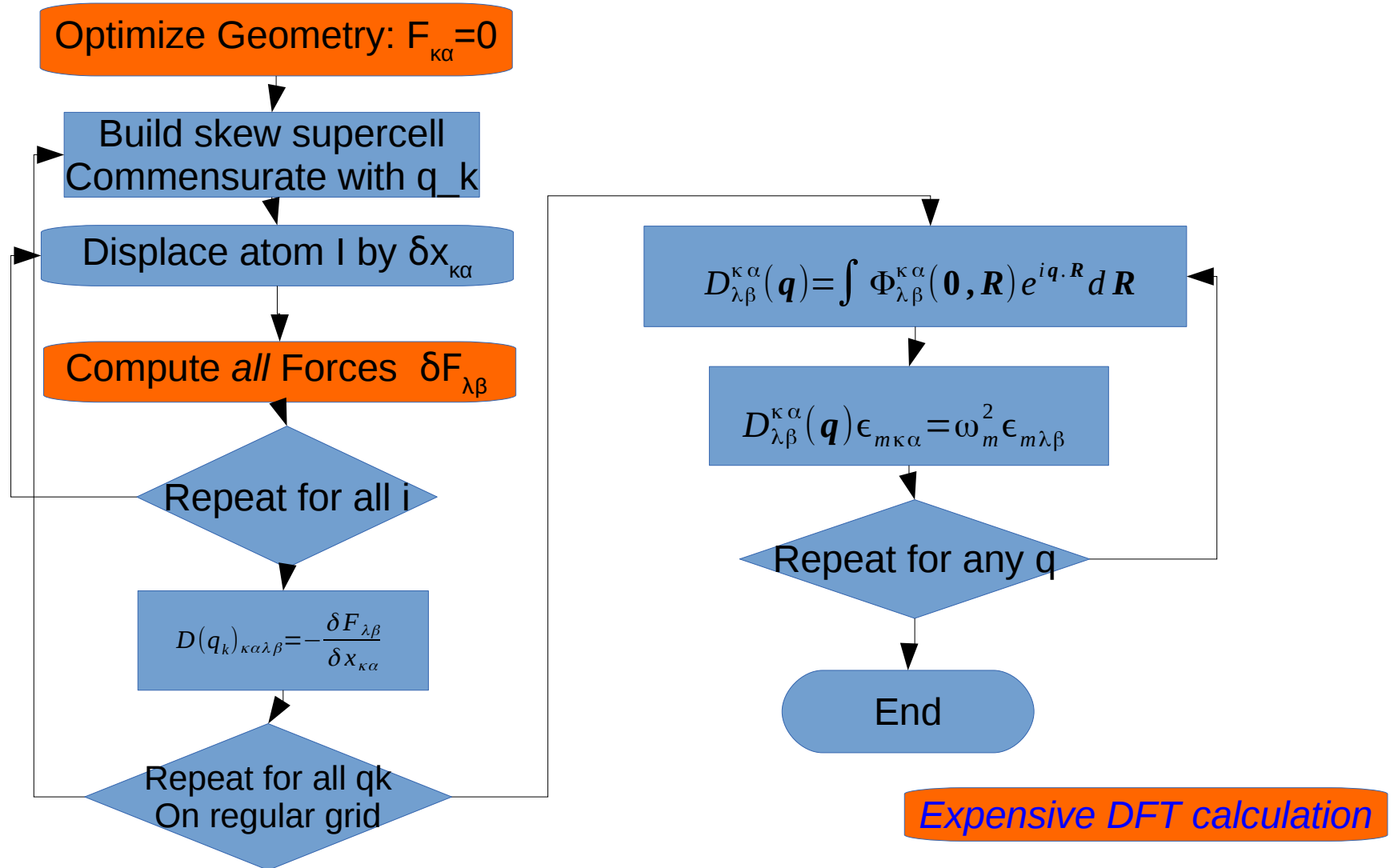
$$D_{\kappa' \alpha'}^{\kappa \alpha}(\mathbf{q}) = \int \Phi_{\kappa' \alpha'}^{\kappa \alpha}(\mathbf{0}, \mathbf{R}) e^{i \mathbf{q} \cdot \mathbf{R}} d\mathbf{R}$$

$$D_{\kappa' \alpha'}^{\kappa \alpha}(\mathbf{q}) \epsilon_{m \kappa \alpha} = \omega_m^2 \epsilon_{m \kappa \alpha}$$

The Supercell Method



The Nondiagonal Supercell Method



Modelling the spectrum

Orientationally averaged infrared absorptivity

$$I_m = \left| \sum_{\kappa, b} \frac{1}{\sqrt(M_\kappa)} Z_{\kappa, a, b}^* u_{m, \kappa, b} \right|^2$$

Raman cross section

$$I_{\text{raman}}^m \propto |\mathbf{e}_i \cdot \mathbf{A}^m \cdot \mathbf{e}_s|^2 \frac{1}{\omega_m} \left(\frac{1}{\exp(\hbar \omega_m / k_B T) - 1} + 1 \right)$$

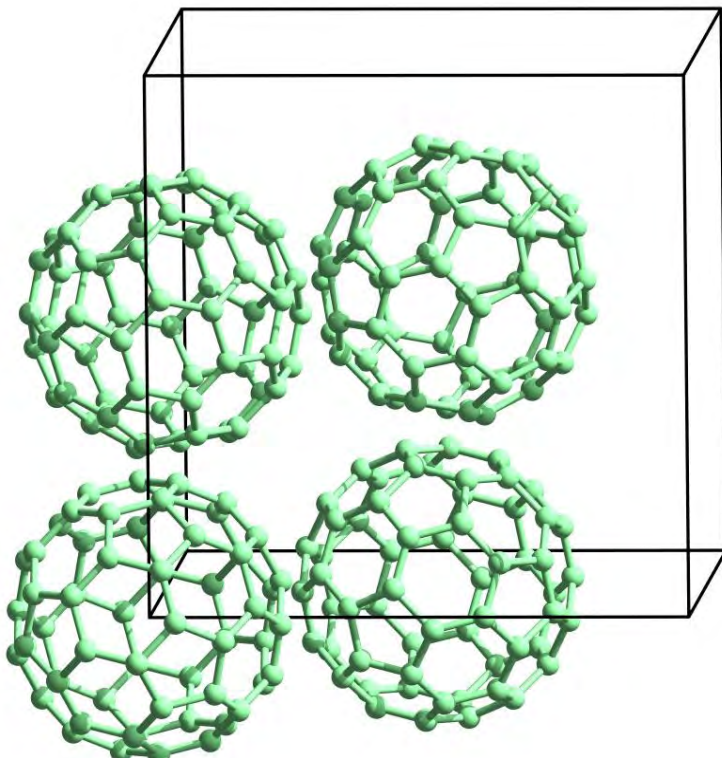
$$A_{\alpha, \beta}^m = \sum_{\kappa, \gamma} \frac{\partial^3 E}{\partial \varepsilon_\alpha \partial \varepsilon_\beta \partial u_{\kappa, \gamma}} u_{m, \kappa, \gamma} = \sum_{\kappa, \gamma} \frac{\partial \epsilon_{\alpha \beta}}{\partial u_{\kappa, \gamma}} u_{m, \kappa, \gamma}$$

Inelastic neutron cross section

$$S^n(\omega_m) = \int dQ \sum_{\kappa} \sigma_{\kappa} \left\langle \frac{(Q \cdot u_{m, \kappa})^{2n}}{n!} \exp(-(Q \cdot u_{m, \kappa})^2) \right\rangle$$

Spectral response to light depends on response of electrons; for neutrons only nuclei.

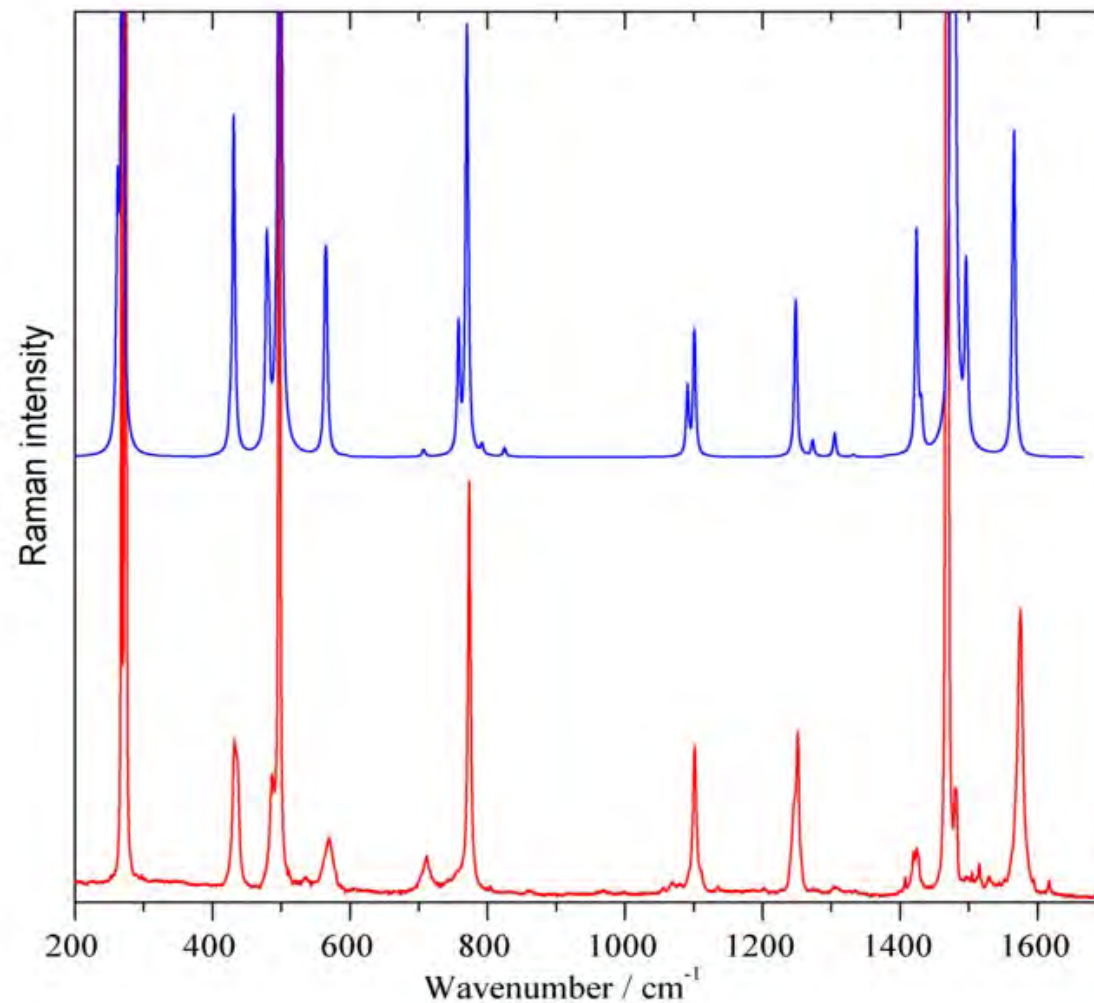
Vibrational spectroscopy of C₆₀



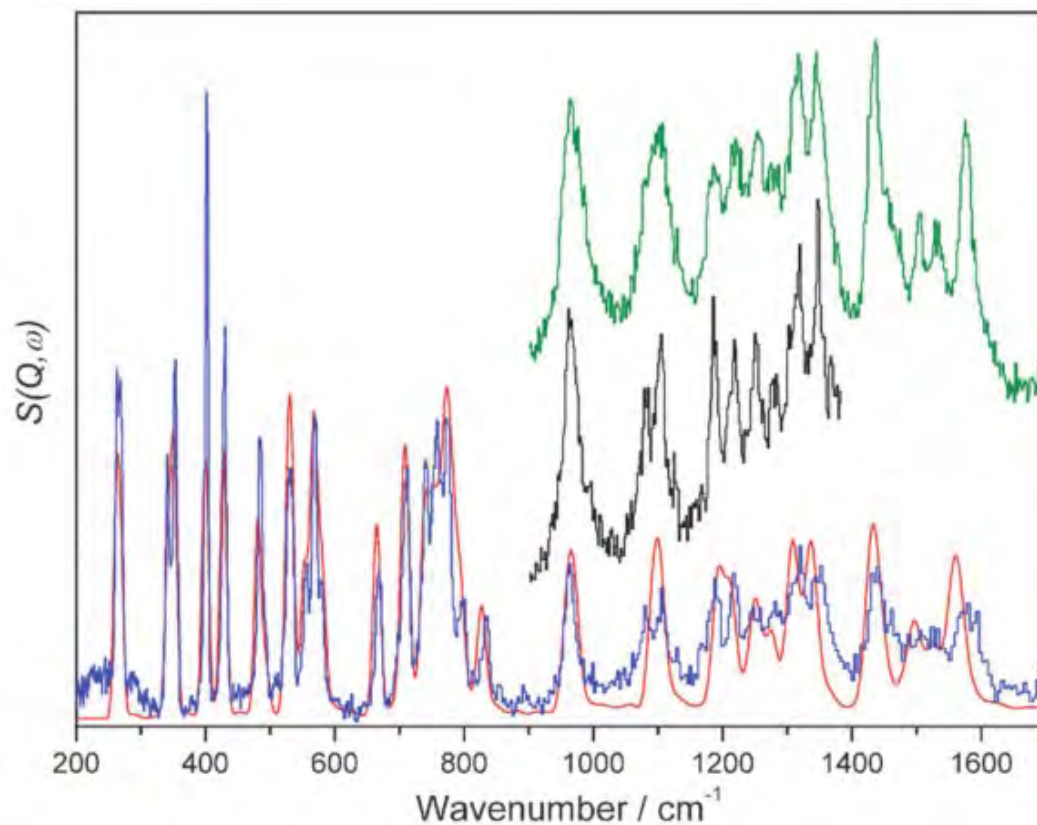
- Above 260K takes Fm3m structure with dynamical orientational disorder
- m3m point group lower than I_h molecular symmetry
- Selection rules very different from gas-phase.
- Intramolecular modes and factor group splitting seen.
- Try ordered Fm3 model for crystal spectral calculation.

Parker et al, PCCP **13**, 7780 (2011)

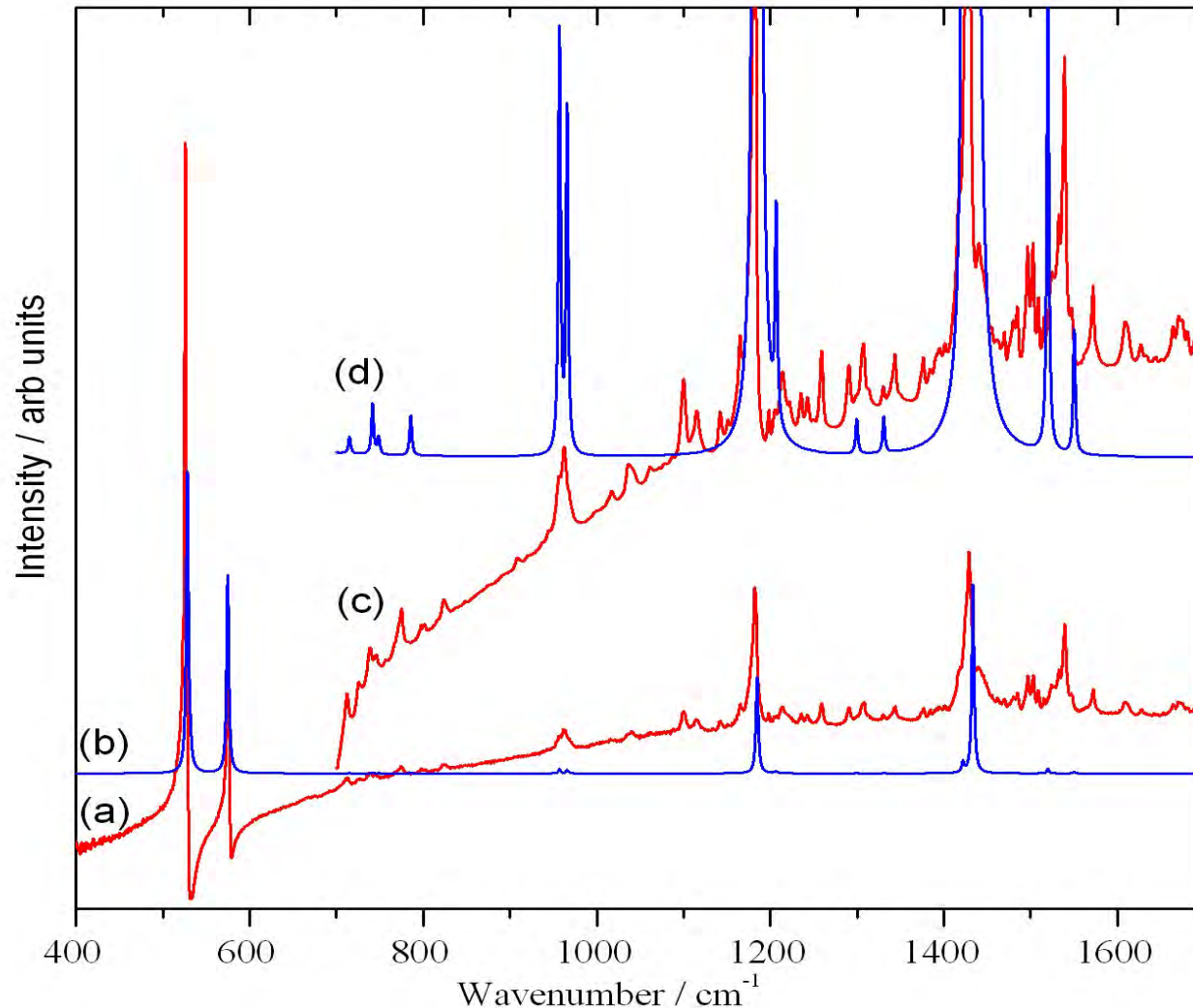
GGA Raman spectrum of C₆₀



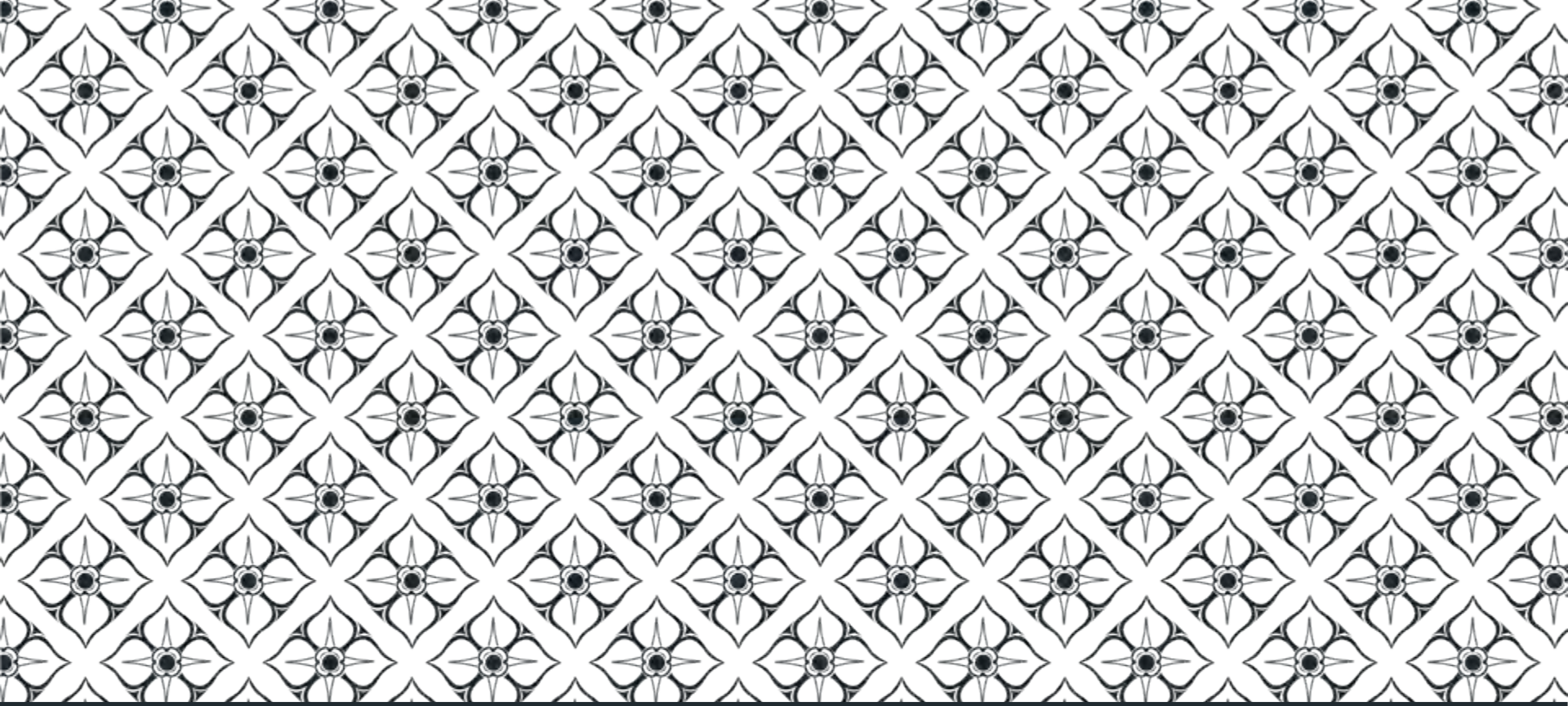
C_{60} INS -Tosca



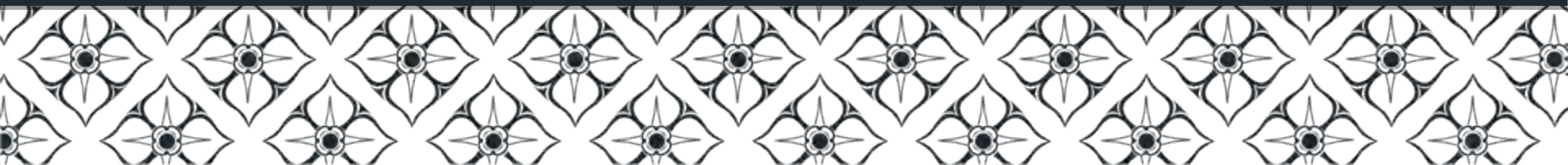
GGA infrared spectrum of C_{60}



Thermoelectric Heat Recovery

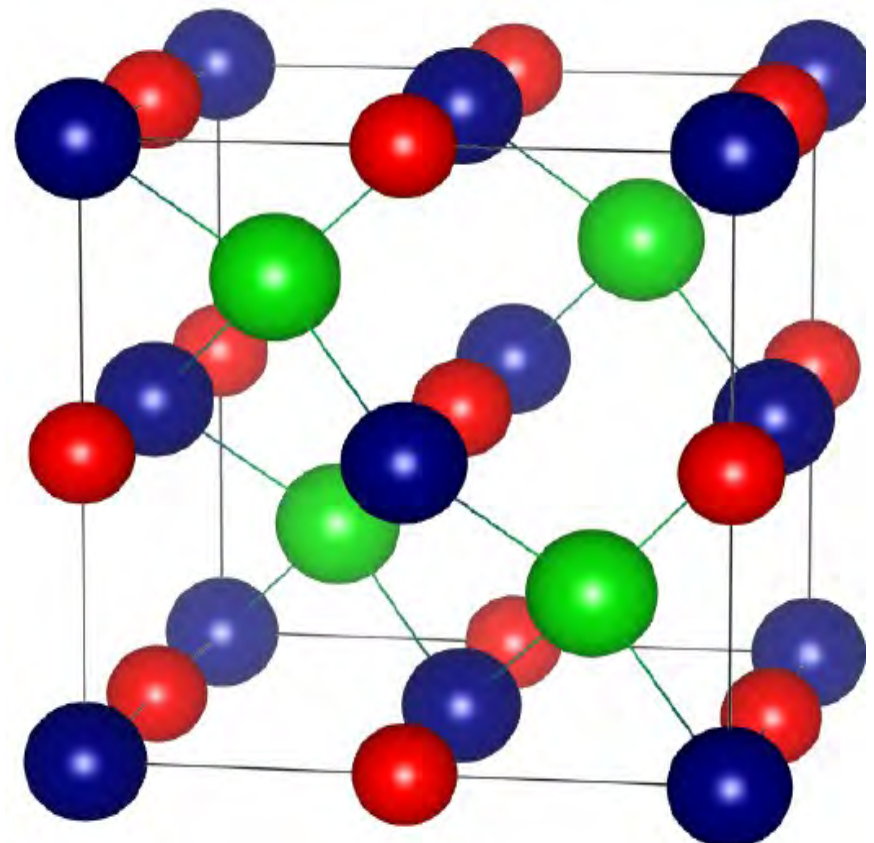


TiNiSn-based Half-Heusler Alloys



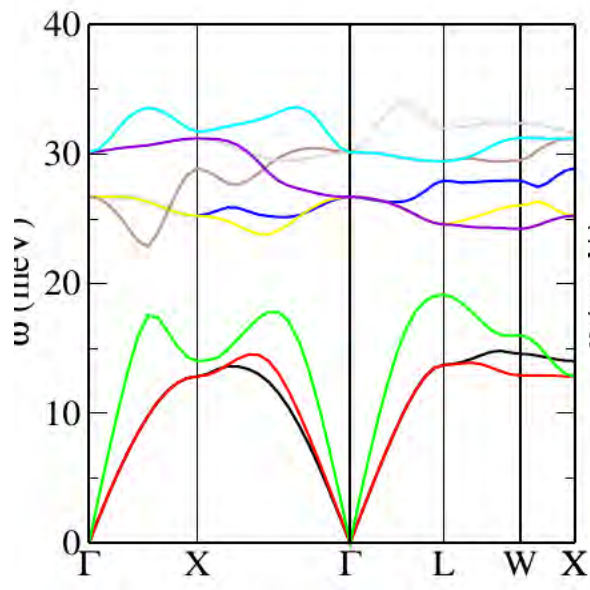
The Half-Heusler Crystal Structure

- Chemical Formula ABC
- A, B, C are elemental metallic elements
- Closed-shell “18-electron” results in insulating band-gap.
- TiNiSn with excess Ni or Cu show high thermoelectric ZT.
- Investigate phonon origin of low thermal conductivity.
- MARI experiments performed on on Ti/Zr/Hf NiSn
- MARI experiments on excess Ni and Cu in TiNiSn

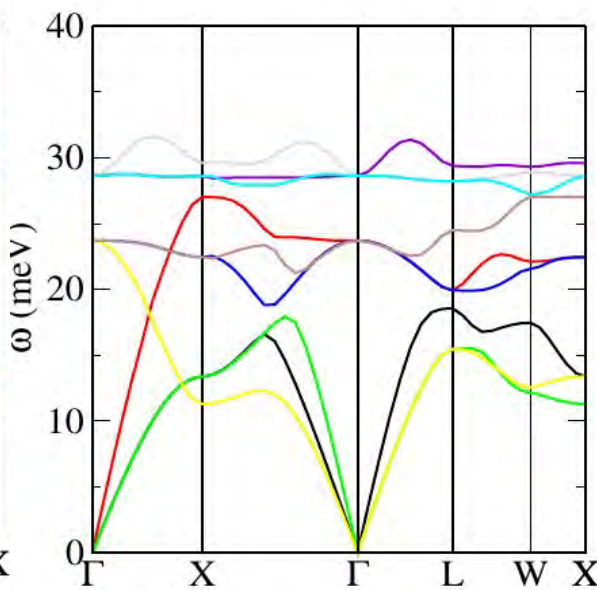


Ti/Zr/Hf series

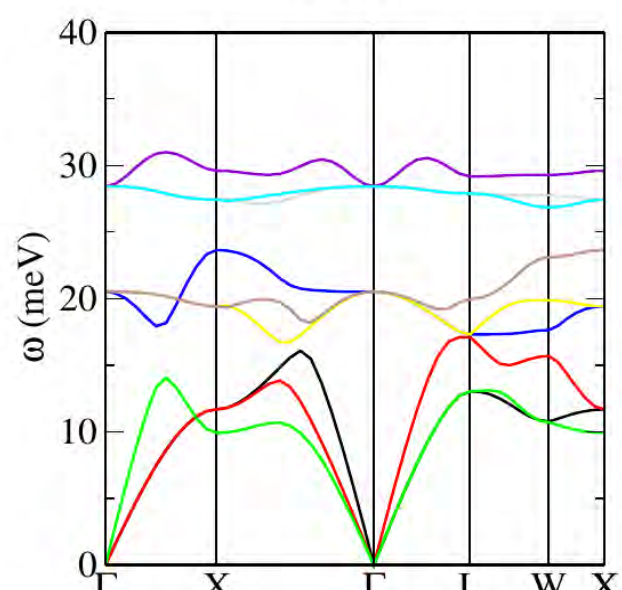
TiNiSn



ZrNiSn



HfNiSn

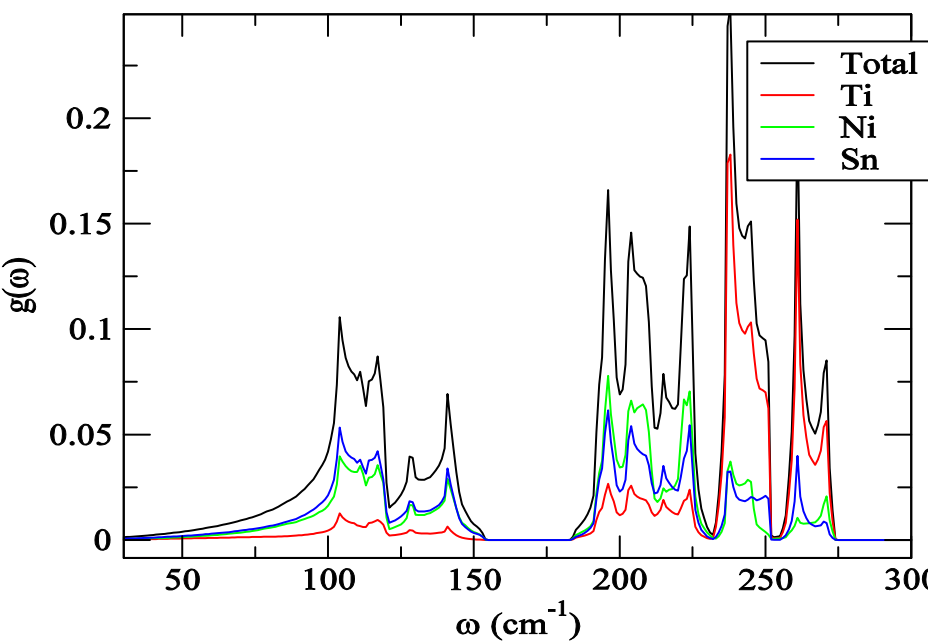


Effect of Excess Ni in TiNiSn

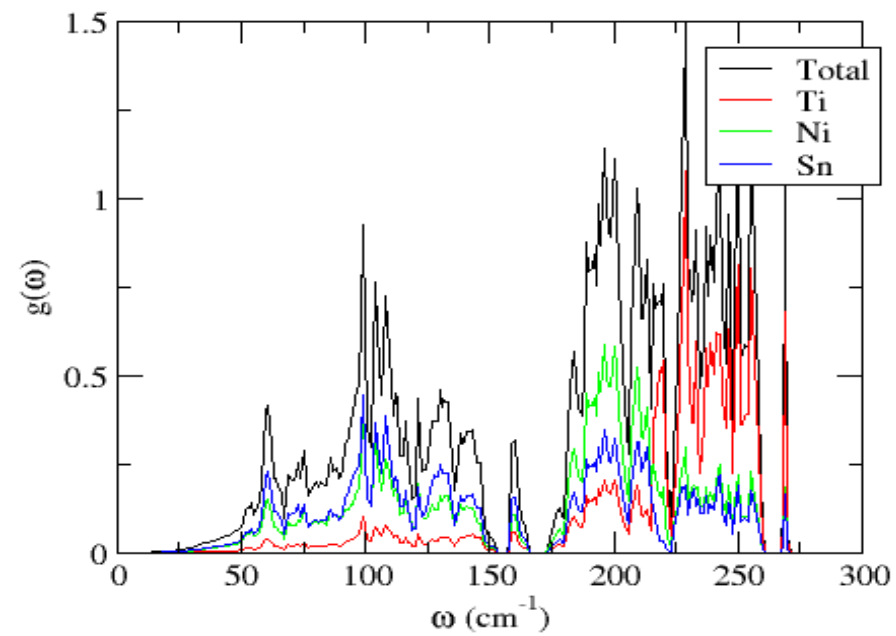


ROYAL
HOLLOWAY
UNIVERSITY
OF LONDON

TiNiSn_dos



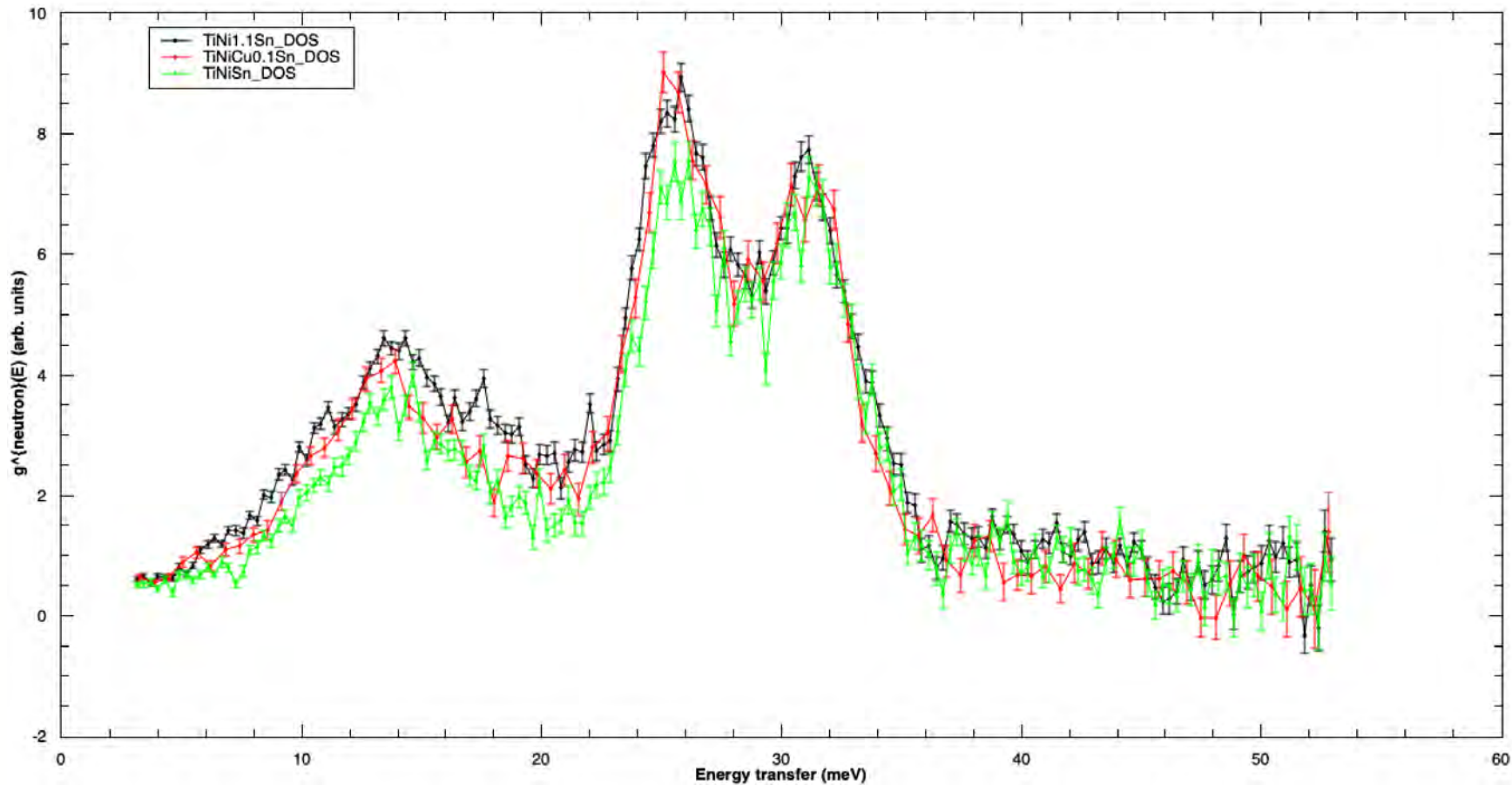
TiNi1.125Sn_dos



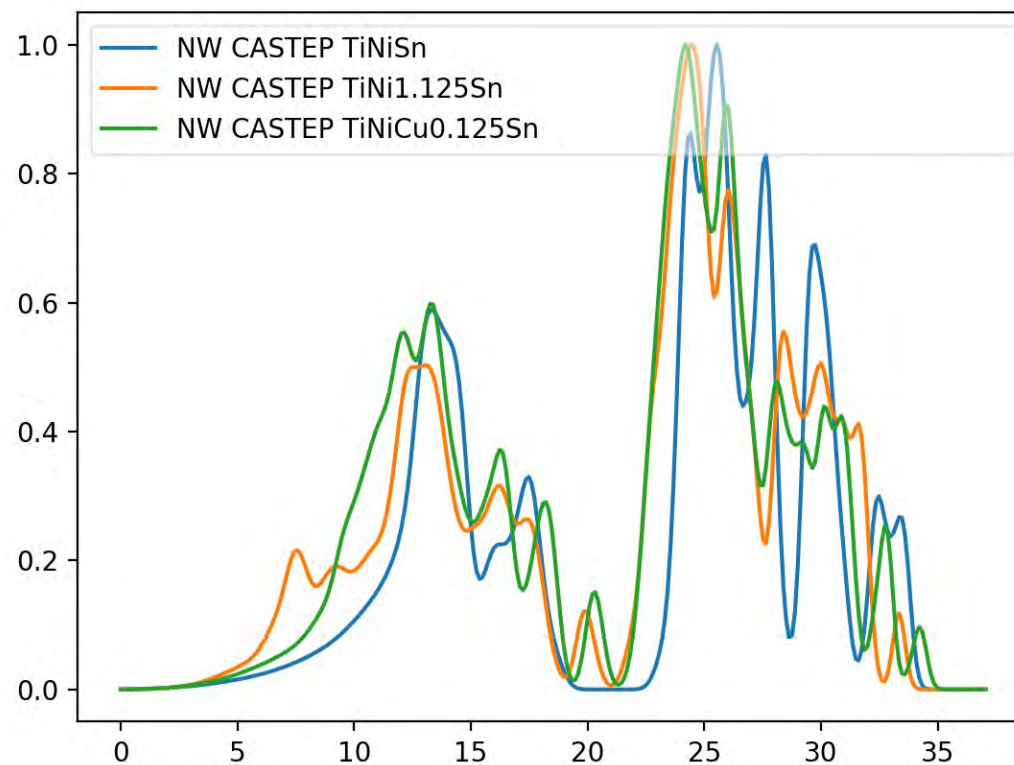
MARI TiNiSn, TiNi1.1Sn, TiNiCu0.125Sn



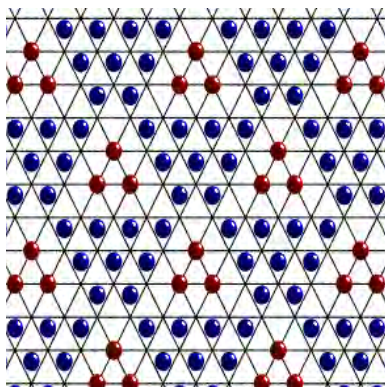
ROYAL
HOLLOWAY
UNIVERSITY
OF LONDON



Neutron Weighted Phonon DOS

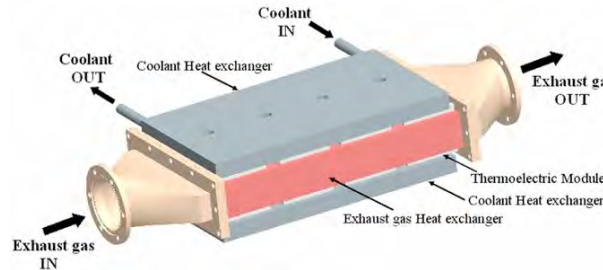


Rattler mode in thermoelectric $\text{Na}_{0.8}\text{CoO}_2$



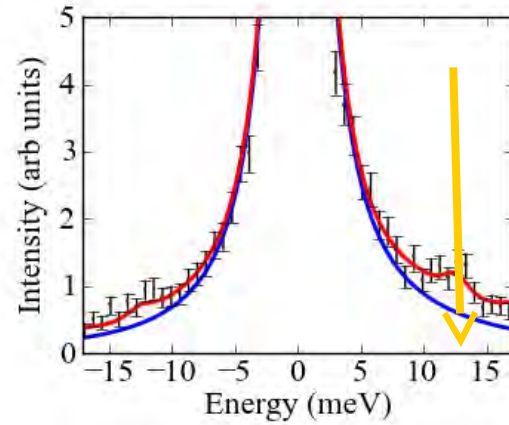
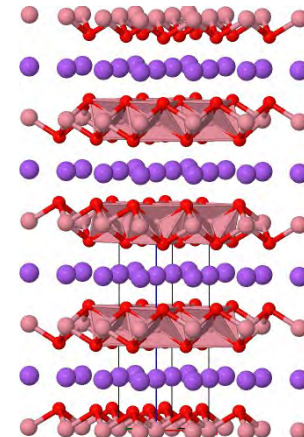
“Square Phase” Na ordering at 150K

Roger, M., et al., Patterning of sodium ions and control of electrons in sodium cobaltate. Nature **445**, 631 (2007)



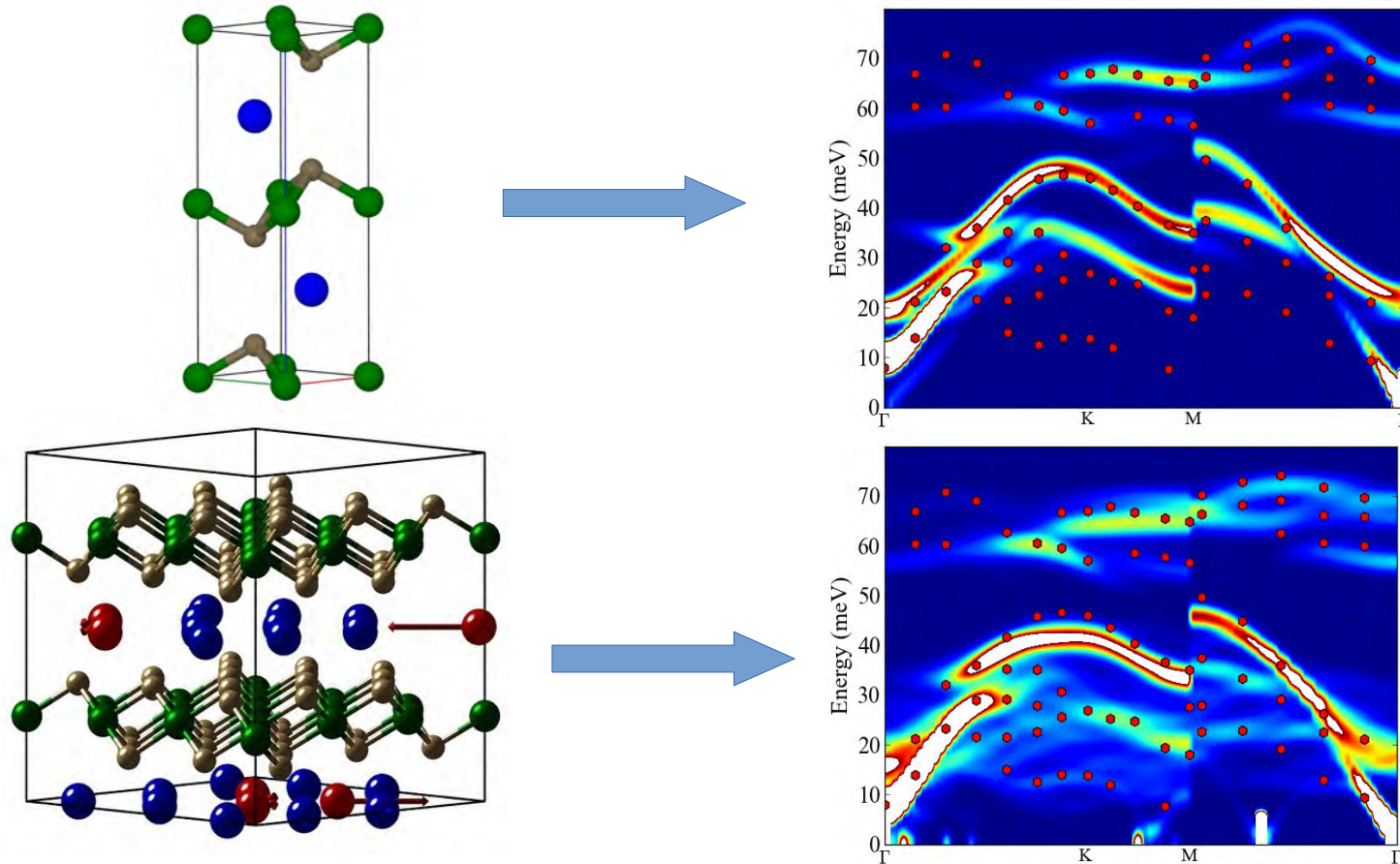
Thermoelectric
“figure of merit”

$$zT = \frac{S^2 T \sigma}{\kappa}$$



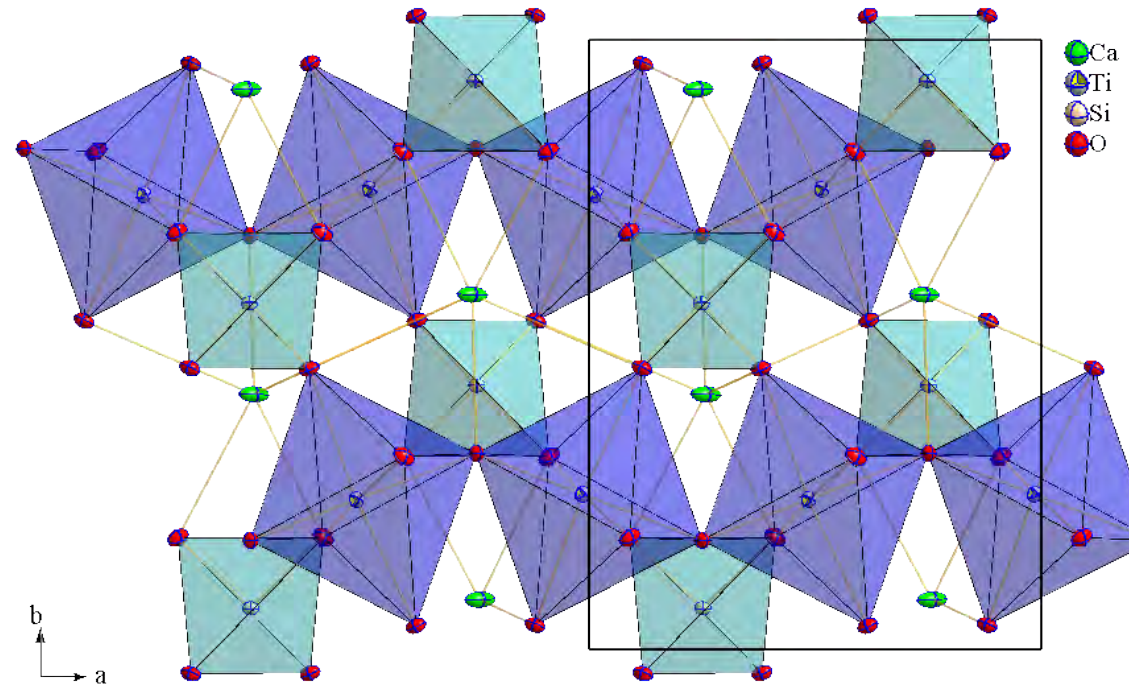
Inelastic X-Ray spectrum
measured at ESRF

Ab initio Lattice Dynamics

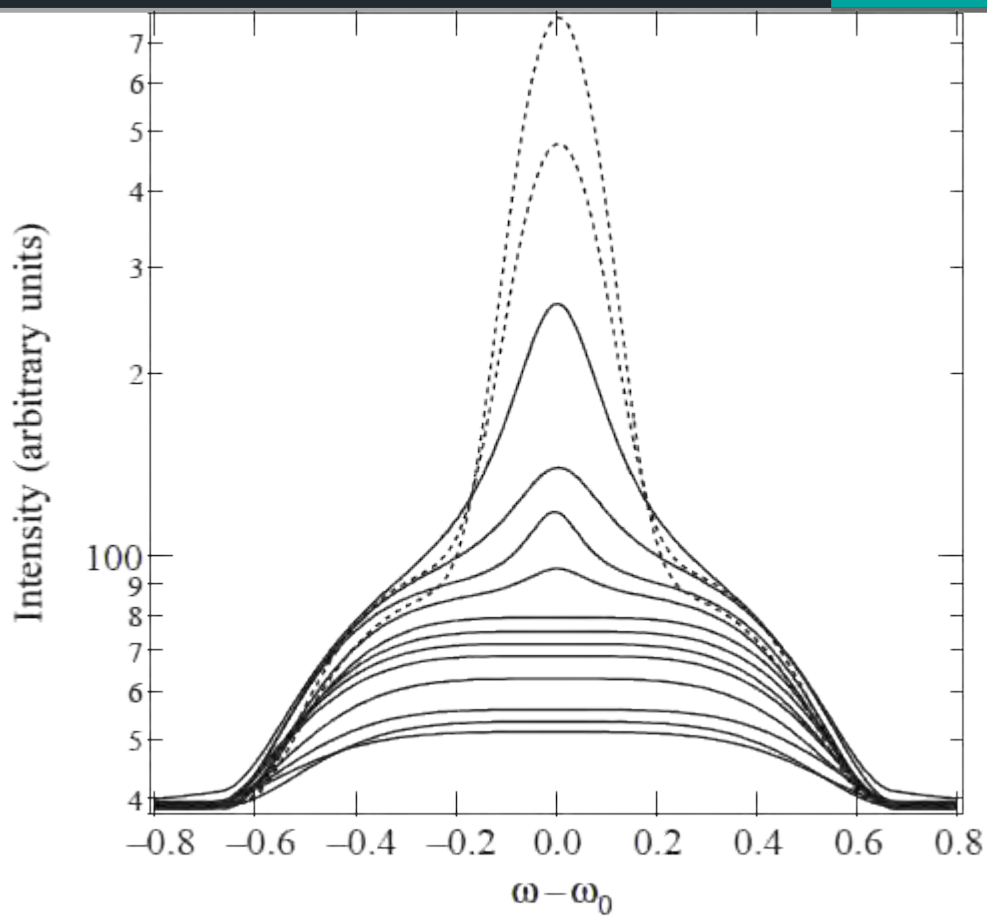
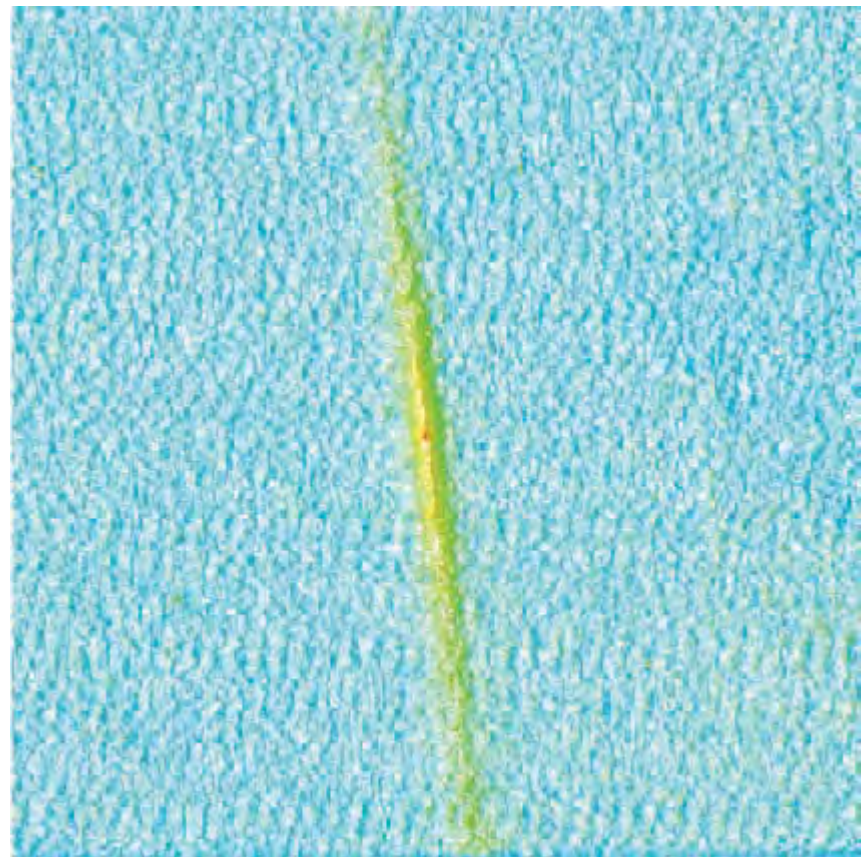


D. Voneshen et al., *Suppression of thermal conductivity by rattling modes in thermoelectric sodium cobaltate*. Nature Materials **12**, 1028 (2013)

Thermal Diffuse Scattering in Titanite



Motivation

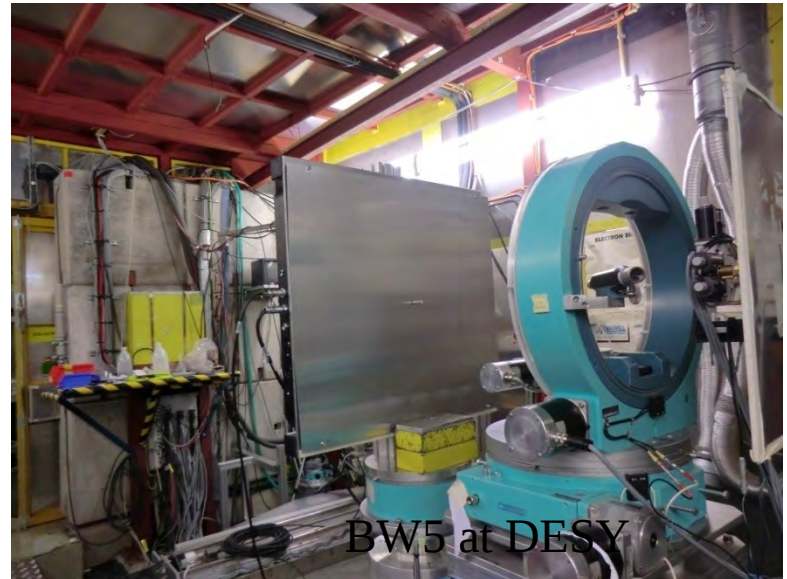


T. Malcherek *et al.*, J. Appl. Cryst. **34** (2001), 108.

Experiment



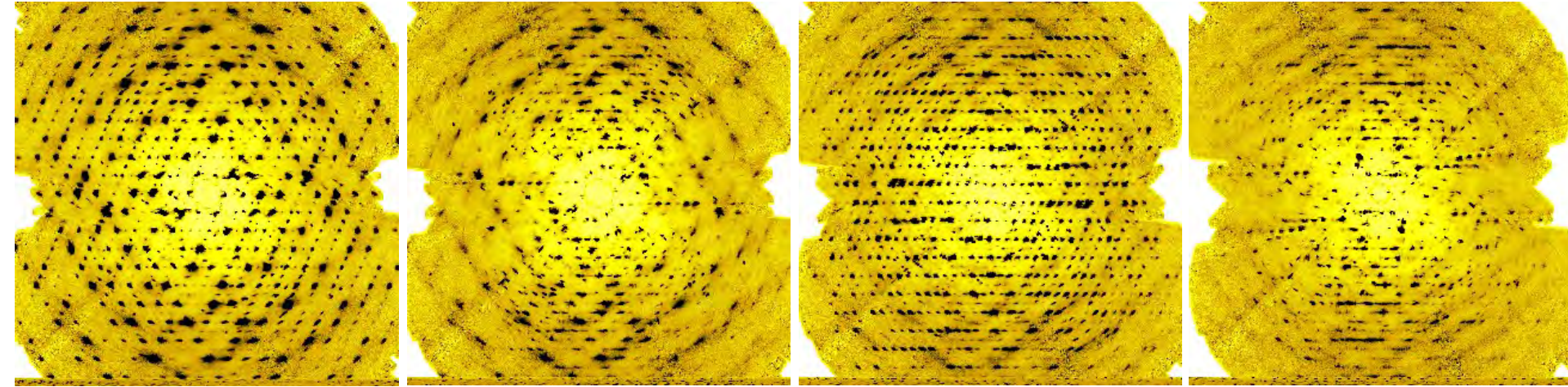
SXD at ISIS



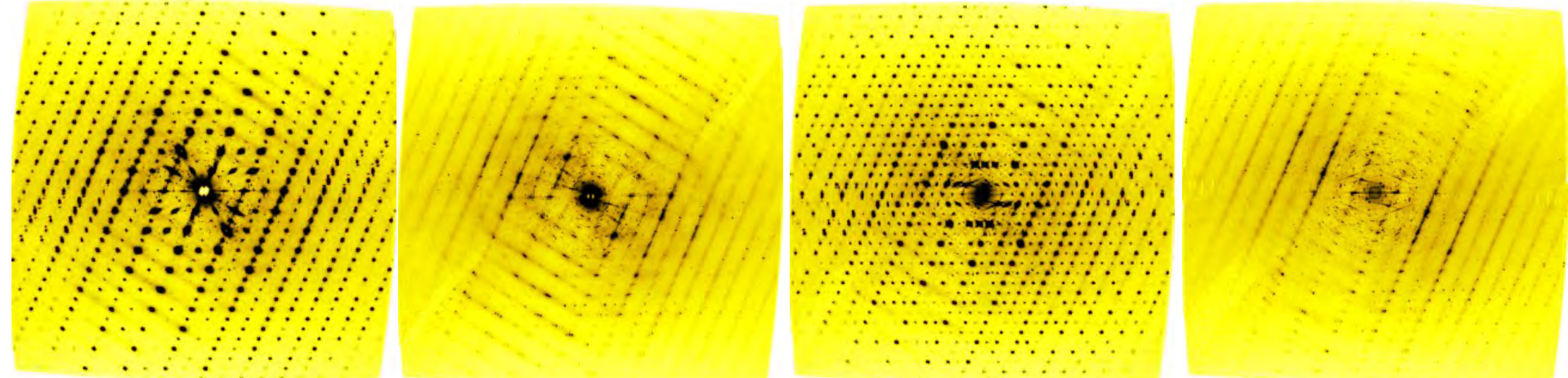
BW5 at DESY



Diffuse scattering



Neutron



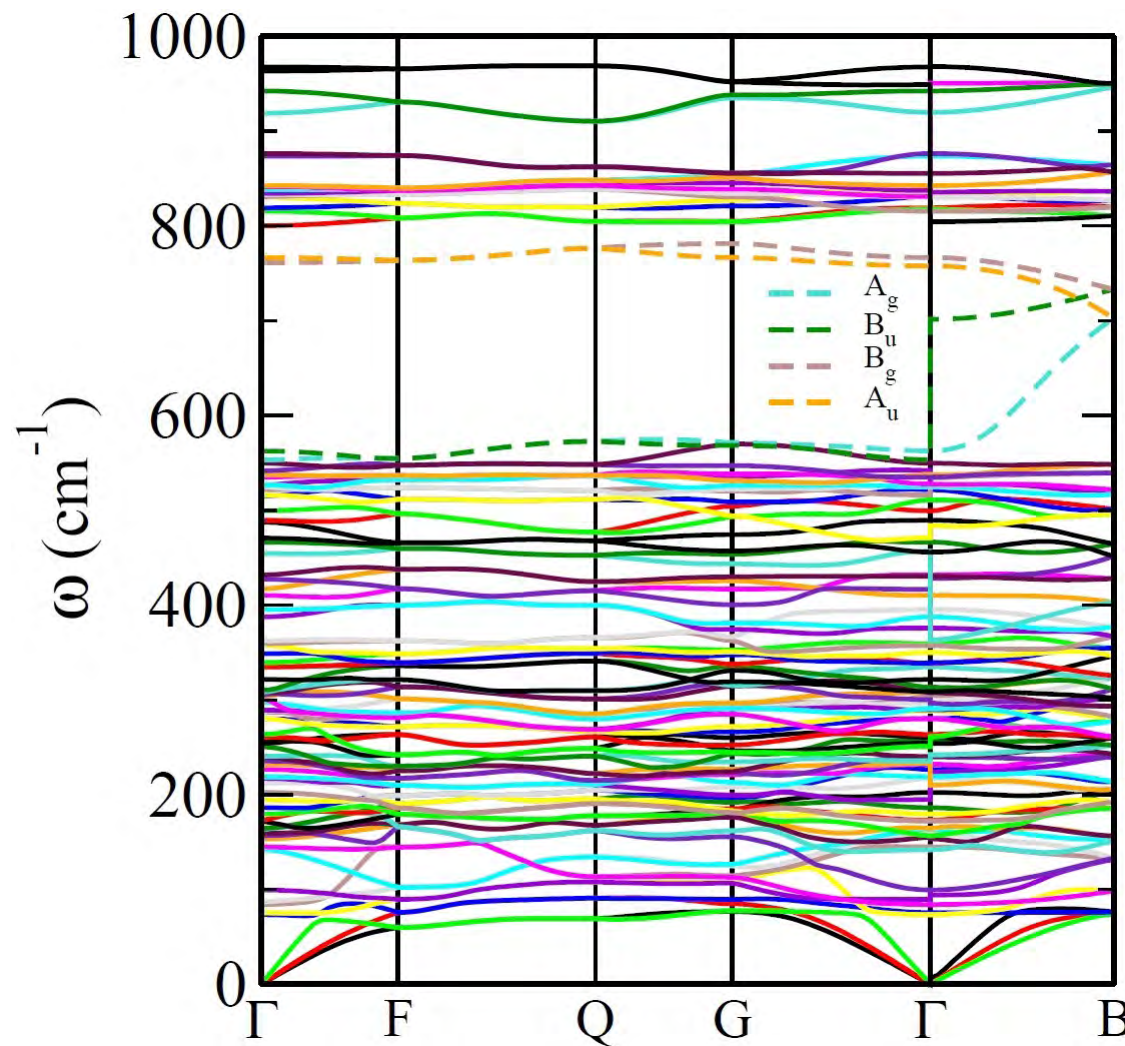
X-Ray

Phonons and diffraction

$$F_j(\vec{q}) = \sum_s \frac{f_s}{\sqrt{\mu_s}} \cdot e^{-M_s \cdot (\vec{q} \cdot \vec{e}_{\vec{q}, j, s})} \cdot e^{-i \vec{q} \cdot \vec{r}_s}$$

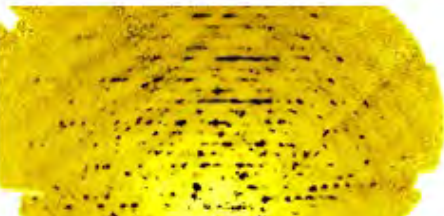
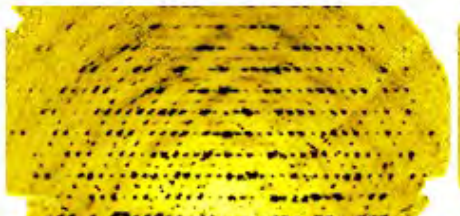
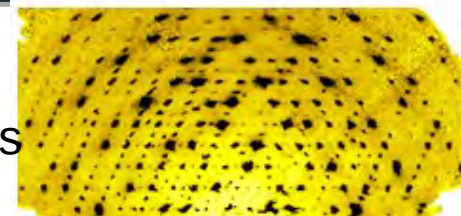
$$I_{TDS} = \frac{\hbar N I_e}{2} \sum_j \frac{1}{\omega_{\vec{q}, j}} \coth \left(\frac{\hbar \omega_{\vec{q}, j}}{k_B T} \right) |F_j(\vec{q})|^2$$

Dispersion curves from DFPT

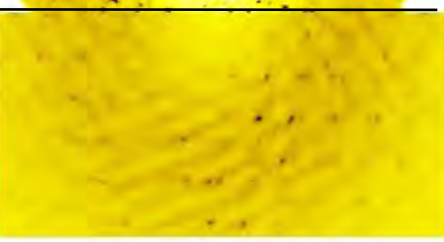
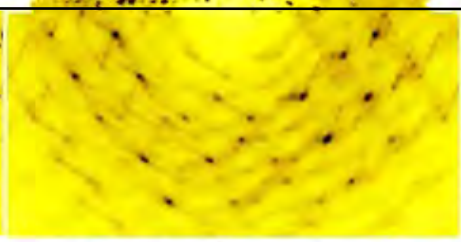
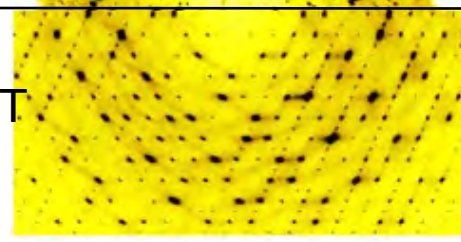


Comparison with data

Obs

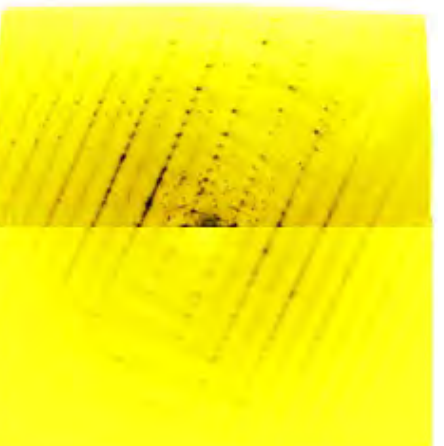
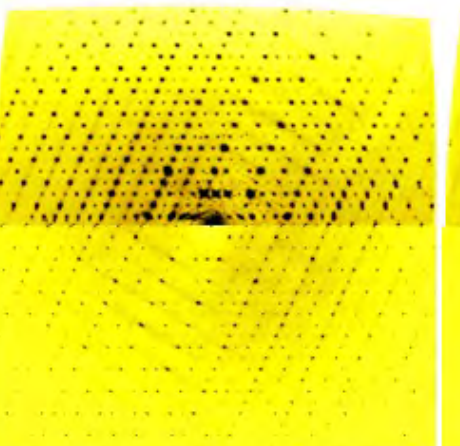
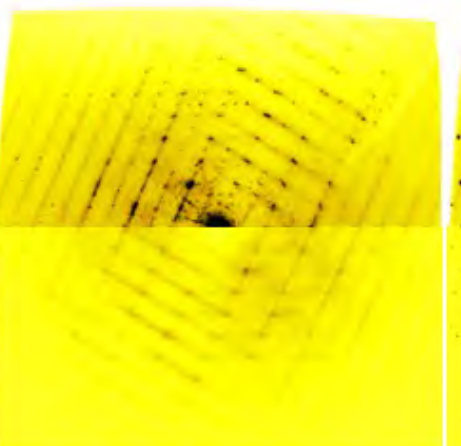
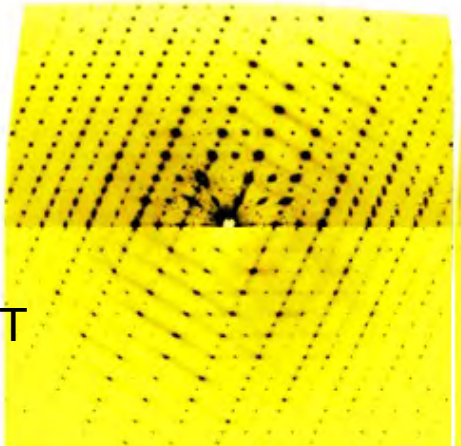


DFT



Neutron

Ob



DFT

X-Ray